

# ARTIFICIAL PHANTASIA: EVIDENCE FOR PROPOSITIONAL REASONING-BASED MENTAL IMAGERY IN LARGE LANGUAGE MODELS

**Anonymous authors**

Paper under double-blind review

## ABSTRACT

This study offers a novel approach for studying complex cognitive behavior in artificial systems. Almost universally, Large Language Models (LLMs) perform best on tasks which may be included in their training data and can be accomplished solely using natural language, limiting our understanding of their emergent sophisticated cognitive capacities. In this work, we created dozens of novel items of a classic mental imagery task from cognitive psychology. The task consists of following a series of short instructions (3-5 steps), performing basic transformations on imagined letters and simple shapes to create a mental image of an object, and finally recognizing and labeling the object. Traditionally, cognitive psychologists have argued that this task is solvable exclusively via visual mental imagery (i.e., language alone would be insufficient). LLMs are perfect for testing this hypothesis. First, we tested several state-of-the-art LLMs by giving text-only models written instructions and asking them to report the resulting object after performing the transformations in the aforementioned task. Then, we created a baseline by testing 100 human subjects in exactly the same task. We found that the best LLMs performed significantly above average human performance (9.4%-18.2% increase over the human average of 54.7%,  $p < .00001$ ). Finally, we tested reasoning models set to different levels of reasoning and found the strongest performance when models allocate greater amounts of reasoning tokens. These results provide evidence that the best LLMs may have the capability to complete imagery-dependent tasks despite the non-pictorial nature of their architectures. Our study not only demonstrates an emergent cognitive capacity in LLMs while performing a novel task, but it also provides the field with a new task that leaves lots of room for improvement in otherwise already highly capable models. Finally, our findings reignite the debate over the formats of representation of visual imagery in humans, suggesting that propositional reasoning (or at least non-imagistic reasoning) may be sufficient to complete tasks that were long-thought to be imagery-dependent.

## 1 INTRODUCTION

Large Language Models (LLMs) have progressed exponentially in the last few years. However, the most popular benchmarks rely on reading comprehension (Kočiský et al., 2018), information recall (Rein et al., 2023; Hendrycks et al., 2021), logical reasoning (Wang et al., 2024b), coding (Khan et al., 2023), or other similar tasks in principle solvable only through text and prone to data contamination risks from preexisting information in their training dataset (Sainz et al., 2023). In recent months, questions about the scalability of complexity, the appropriate usage of reasoning tokens, and the design and evaluation of reasoning tasks have been raised despite LLMs performance (Shojaee et al., 2025; Lawsen, 2025). Here, we present a mental imagery task adapted from cognitive psychology that offers an opportunity for assessing models in novel and sophisticated ways. We designed bespoke stimuli that we can be certain are not in their training data and that, as we show below, leave room for great improvement in models' performance (despite the best models outperforming humans). Moreover, our results suggest that LLMs may be capable of performing a mental imagery task long-thought to be unsolvable by relying solely on language, offering a new challenge for cognitive psychology.

## 1.1 PICTORIAL VS. PROPOSITIONAL MENTAL IMAGERY

Cognitive psychologists have been embattled in the last fifty years in a heated debate about the nature of mental imagery. Two opposing camps have proposed that mental imagery’s format is either pictorial (e.g., Kosslyn (1973; 1996)) or propositional (e.g., Pylyshyn (1973; 2002)). In general, a propositional format would be one in which the representation is composed of discrete symbolic elements that can be combined to create new, complex representations (e.g., the word “red” and the word “house” are discrete symbols that, when combined, can create the complex representation “red house”). Advocates of the propositional view argue that the visual information contained in mental images can be captured by propositional descriptions (i.e., discursive elements) in a symbolic so-called “language of thought”. In consequence, tasks used to prove mental images are in a pictorial format can all, after all, be solved through language or reasoning alone. Pictorialists disagree. They consider some representations are non-symbolic and non-discrete: analogue, continuous representations that do not have a canonical decomposition (e.g., “red house” is naturally parsed as “red” plus “house”, but how are we to systematically parse the many strokes of the Mona Lisa?). Rather, parts of pictorial mental representations correspond to parts of what they represent and they represent multiple properties simultaneously (Quilty-Dunn, 2019).

One of the foundational studies of pictorial mental imagery is an object reconstruction task (Finke et al., 1989). Subjects were required to visualize in their mind’s eye a series of combinations and transformations of basic shapes and letters. Subjects then indicated what object the resulting construction of shapes looked like in a free verbal report. The structure of this task is straightforward. Simple shapes and letters are given in stages to the subject where transformations of the existing figures (or the entire scene) follow (Figure 1). Between 2 and 4 sets of transformation instructions are provided before the subject is asked to identify the final image.

The pictorial view of mental imagery vastly dominates psychology today (Pearson & Kosslyn, 2015; Pearson et al., 2015; Block, 2023; Zeman, 2024). According to it, success in this task (and others like it) is only possible through the use of visual pictorial imagery (as opposed to logical or propositional reasoning, but see Pylyshyn (2002)). The pictorial view has gained dominance in the field through its appeal to evidence from neuroimaging studies showing similarities in neural activity between visual and imagery tasks (Pearson et al., 2015; Naselaris et al., 2015; Dijkstra et al., 2019) and, crucially, from mental imagery tasks (Shepard & Metzler, 1971; Kosslyn, 1973; Finke et al., 1989; Pearson & Kosslyn, 2015). For example, in the Finke et al. object reconstruction task, the final identification step is supposed to require a properly constructed *image* that subjects can simply read off from their mind’s eye. Confidence in this view is so strong that some proponents go as far as to think that solving this kind of visualization tasks is “virtually impossible to do without using [pictorial] imagery” (Finke, 1990, p. 19).

	Step 1	Step 2	Step 3
Instructions	Imagine a capital letter “D”.	From there, imagine the figure rotated 90 degrees to the left.	From there, imagine a capital letter “J” attached to the bottom center of the figure.
Mental Image			

Figure 1: One of the instruction sets introduced in Finke et al. (1989). Here, subjects are meant to recognize from the resulting mental image that the final imagined object looks like an *umbrella*. The instructions have been rewritten to be clearer both for prompting LLMs, as well as for human understandability.

## 1.2 SOLVING MENTAL IMAGERY TASKS WITHOUT MENTAL IMAGERY?

Many tasks in everyday life involve the usage of mental imagery to some degree (e.g., navigation, planning and decision-making, mental simulation, episodic memory, organization, spatial reasoning, emotional engagement and regulation, among others; Bocchi et al. (2017); Shepard & Metzler (1971); Palombo et al. (2018); Wheeler et al. (2000); Byrne et al. (2007); Holmes & Mathews (2010); Krasich et al. (2024)). Unsurprisingly, most humans report having conscious mental imagery. However, a small percentage (1-4%) of the population—aphantasics—report no conscious mental imagery (Wright et al., 2024; Faw, 2009; Zeman et al., 2015; Dance et al., 2022; Zeman, 2024). If the pictorial view were correct, we would predict aphantasics to be incapable of performing mental imagery tasks at all; but this is not what we find (Blomkvist, 2023; Kay et al., 2024; Pounder et al., 2022; Bainbridge et al., 2021). Aphantasics perform (almost) at the same level as people with imagery. While there is a possibility that they rely on unconscious visual mental imagery (Nanay, 2021; Michel et al., 2025), aphantasics tend to report that they use verbal strategies (Keogh et al., 2021; Kay et al., 2024), giving renewed credence to the possibility of a purely propositional mental imagery.

In the human mind, language and imagery are deeply intertwined. It can be hard to evaluate the introspective reports of subjects (aphantasic or not) about the strategies that they use, as humans in general do not have good access to the inner processes that support their behavior (Nisbett & Wilson, 1977); or they may confabulate about the actual contents of their mental images (Bigelow et al., 2023). State-of-the-art artificial systems such as LLMs offer a unique opportunity to test a system whose architecture and processing is primarily propositional, specifically, linguistic. Nothing truly analogous to a visual (i.e., pictorial) mental imagery seems available to LLMs.<sup>1</sup> Does this mean that there are types of reasoning that are just not available to them? Or is it possible that LLMs rely solely on their language-trained and language-processing architecture to achieve similar goals as humans who experience mental images? After all, as mentioned earlier, aphantasics are reported to perform at the same levels as imagers in a plethora of tasks previously thought to require mental imagery. The imagery debate does not seem, after all, to have been completely settled.<sup>2</sup>

## 1.3 MOTIVATION FOR LLM MENTAL IMAGERY TASKS

To test whether LLMs are capable of solving tasks designed to probe pictorial mental imagery despite relying exclusively on text processing, we gave several state-of-the-art models (Claude, Gemini, OpenAI), as well as several open-weight models (DeepSeek, Qwen, GPT oss), expanded, bespoke instruction sets following Finke et al. (1989)’s approach described above. We also asked models with image capabilities to generate images in each step and to consider them in their answers. As the object reconstruction task we used is compositional (different images or aspects of images from each step need to be combined in subsequent steps to obtain the final answer), we conjectured that image-aided reasoning could increase performance, especially if the pictorial imagery framework is correct, and if forcing the models to produce and consider images in the intermediate steps could alter their approach to the task. (See Appendix C for further discussion about this approach.) Finally, we obtained a human baseline for for this task by testing 100 human subjects.

Whether LLMs can perform at a human level on this task is of intrinsic interest to understand what these new models can achieve. This type of object reconstruction is an ideal challenge for LLMs. The task is structured entirely through natural language (both the input and the output); the results are easily evaluated; and we included newly created examples that could not possibly be in their training set. Moreover, due to the nature of the task and the fact that it can be expanded, a human baseline can be straightforwardly established at any point. Additionally, LLMs performing at or beyond the human baseline would constitute evidence for LLM propositional reasoning-based imagery. The

<sup>1</sup>While recent multimodal extensions have been trained not just on linguistic corpora but on images as well, and they can take images as input and produce them as output, they still rely on high-dimensional embeddings that are not visual in nature Kiela & Bottou, 2014; Kim et al., 2020; Radford et al., 2021. Current models certainly do not have a dedicated visual module built-in and they do not process tokens in a visual format.

<sup>2</sup>Aphantasia research has recently re-opened questions regarding the nature of mental imagery representations (Lorenzatti, 2025; Lebon, 2025). Proposals have ranged from unconscious pictorial representations (Michel et al., 2025; Nanay, 2021) and absent pictorial representations to a preserved spatial imagery despite a diminished or absent object imagery Bainbridge et al., 2021; Phillips, 2025. The door for non-pictorial mental imagery has certainly reopened.

162 results from this task are also of interest for the cognitive science debate about the format(s) of  
 163 mental imagery, since it would put to a test the idea that mental imagery necessarily involves some  
 164 pictorial component.  
 165

#### 166 1.4 RELATED WORK

167  
 168 Recent publications exploring LLMs’ capacities have included notable work on classic cognitive  
 169 tasks, e.g., evaluating spatial cognition as an emergent property of frontier models (Ramakrishnan  
 170 et al., 2025; Wu et al., 2024; Ivanova et al., 2025), or measuring the stability of psychometric  
 171 attributes (Li et al., 2024). Additionally, benchmarks for spatial and visual reasoning have been  
 172 established (Chollet et al., 2025). More broadly, emergent cognitive properties of artificial systems  
 173 have also been studied beyond just those of the transformer architecture. There is a wealth of accu-  
 174 mulating evidence showing that Deep Neural Networks (DNNs) are useful tools for understanding  
 175 human cognition in general (Demszky et al., 2023; McGrath et al., 2024; Leshinskaya et al., 2025;  
 176 Frank & Goodman, 2025) and visual perception in particular (Chen & Bonner, 2025; Yamins et al.,  
 177 2014). Finally, recent attempts to enhance LLMs’ visual reasoning capacity (e.g., spatial planning,  
 178 visual completion) have explored the capabilities of visual-language models (Yang et al., 2025).  
 179 While this last study offers an interesting approach, here we focus on the foundational question of  
 180 whether mental imagery tasks (rather than visual tasks) can be solved by frontier LLMs on the sole  
 181 basis of linguistic manipulation. We discuss several other related topics in Appendix C.

## 182 2 EXPERIMENTAL DESIGN

183  
 184 We used 60 instruction sets for an object recognition task. The set consisted of 48 completely novel  
 185 examples, which we created specifically for this study, and the remaining 12 were taken from the  
 186 original study by Finke et al.. Our new items varied in number of steps (2 to 4), final object, and  
 187 overall complexity (Figure 2). We aimed to keep Finke et al.’s restriction that the final shape should  
 188 not be identifiable until after the final transformation. Some of the tasks resulted in the same (or  
 189 very similar) final shapes (e.g., three different ways of arriving at a shape that represented “glasses”  
 190 or “binoculars”), but as all combinations were unique and involved novel transformations, we  
 191 believe this is not of concern.  
 192

	Step 1	Step 2	Step 3	Step 4
Instructions	Imagine two lowercase letter “o” next to each other.	From there, imagine the two figures pressed together so that they are just touching.	From there, imagine another lowercase letter “o” just touching the top of the figure in the center.	From there, imagine a lowercase letter “v” just touching the bottom of the figure in the center.
Mental Image				

193  
 194  
 195  
 196  
 197  
 198  
 199  
 200  
 201  
 202  
 203  
 204 Figure 2: One of our new instruction sets demonstrating the slightly increased cognitive complexity  
 205 and more ambiguous canonical form (“balloons”, “flower bouquet”, or “ice cream”, among others).  
 206 Note the usage of two letters in the first step, the abstract reference to existing symbols and scenes,  
 207 and the final shape not being determinable until the final step.  
 208

209 Our new items integrated several changes to the original ones developed by Finke et al. (1989).  
 210 Most notably, we allowed one step to include up to two letters, rather than just one, thus increasing  
 211 cognitive load (Miller, 1956; Farrington, 2011) but allowing more varied scenes. Additionally, we  
 212 did not restrict the final image to having only one canonical form. The intended canonical form was  
 213 not always immediately obvious, though at least one form was always clear. Our items’ difficulty  
 214 had a wider range, which we confirmed after establishing a new human baseline (see Appendix  
 215 2.3). The complete instruction-sets are included in the project’s anonymous GitHub repository (see  
 Appendix B).

216 Finally, we updated the language in the 12-items taken directly from Finke et al. to match the format  
217 of our improved versions. Notably, ambiguous language was clarified (e.g., specification of capital  
218 versus lowercase letters), subsequent instructions were modified to reference earlier instructions only  
219 abstractly (e.g., “the existing symbol” versus “the ‘E’”), and 180 degree rotations were changed to  
220 flips (when vertical) or mirroring (when horizontal). We did not ask models or human subjects to  
221 guess the resulting shape at each step, unlike the original experiment, only its final form.

222 We should highlight that because these 48 new items were created *ex novo* for this experiment, it is  
223 highly improbable that any of them were present in the training data of any of the LLMs, and it is  
224 materially impossible that all of them were. This is of crucial importance for testing the emerging  
225 reasoning capacities of these types of models.

## 227 2.1 IMAGE-AIDED INSTRUCTIONS

228  
229 For each model that had a compatible image generation pipeline (excluding GPT-5<sup>3</sup>), we ran a  
230 modified version (Image-Aided) of the standard version (Language-Only) described above. In this  
231 modified image-aided version, models were prompted to generate images and modify those images  
232 (see Supplemental Figure S1 for an example), rather than imagine. Whenever possible, we kept  
233 reasoning enabled within the models. For Gemini we used the native image generation capabilities  
234 of 2.0 Flash’s image generation preview version, and, for OpenAI, we used the native GPT-image-1  
235 image generation tool integration.

## 237 2.2 MODEL SELECTION

238  
239 We gave the 60 instruction sets to three consumer accessible groups of models: Claude, Gemini,  
240 and OpenAI. For OpenAI reasoning models, ‘reasoning’ was enabled and ‘reasoning\_effort’ set to  
241 ‘high’. For older Gemini models, ‘thinking’ was set to ‘dynamic’. For Gemini 3 Pro, ‘thinkinglevel’  
242 was set to ‘high’. For Claude Sonnet 4 we allocated 4000 tokens for extended thinking; for Claude  
243 Opus 4.1 we allocated 9000. For models that allow temperature modification, the value was set to  
244 0.1 (we discuss some impacts of this in Appendix E.3). All other parameters were kept at default  
245 values. Our specific model choices are outlined in Supplemental Table S1.

246  
247 For our initial analysis, we performed each experiment twice: once in a single context for all instruc-  
248 tion sets (single-context), and once with a new context for each instruction set (multiple-context).  
249 This was done to see whether there was any significant difference in performance due to in-context  
250 learning (Dong et al., 2024; Wurgaft et al., 2025). The instruction sets were presented to each model  
251 in the same random order.

252  
253 After completing our testing of the proprietary consumer models, we further tested four open-weight  
254 models: Qwen 3, Qwen 3 VL, DeepSeek R1, and gpt-oss-120b. We left all parameters to their  
255 default specifications, with exception of the ‘reasoning\_level’ parameter for gpt-oss-120b which we  
256 set to ‘high’.

## 258 2.3 HUMAN BASELINE

259  
260 We recruited 100 adult participants online. Each was given a random subset of 15 of the 60 instruc-  
261 tion sets (Finke et al. sets and our 48-Item expansion set) for a total of 1500 submitted answers.  
262 Each instruction set had between 21-27 responses. The instruction sets were administered through  
263 a Qualtrics XM survey in a random order. To prevent textual biases from impacting the results (e.g.,  
264 seeing a ‘d’ on a screen affecting the specific shape of the imagined ‘d’), the instructions were played  
265 through audio recordings. Each occurrence of a letter in an instruction was modified to include the  
266 corresponding phonetic word from the International Radiotelephony Spelling Alphabet to increase  
267 the clarity of individual instructions (e.g., “Imagine a B, as in Bravo.”). All audio was recorded by  
268 the same speaker (Author ‘Anonymous’) and there was only one version of each audio instruction.  
269 If the same instruction appeared in two different sets, each set was given unique recordings. Partic-  
270 ipants were able to listen to the instructions as many times as needed, and were asked to imagine

---

268 <sup>3</sup>GPT-5 was released after we collected data on our image paradigm and found that it did not succeed for  
269 other models. As no further upgrades for GPT-image-1 were additionally released we chose not to test GPT-5  
with GPT-image-1.

270 shapes without any visual aids (e.g., drawing). Finally, participants completed the Vividness of Vi-  
 271 sual Imagery Questionnaire (VVIQ) to assess their overall mental imagery capacity (Marks, 1973)  
 272 (see Appendix D.3). Subjects participated for payment and were recruited through the online plat-  
 273 form Prolific with an evenly distributed gender quota. To ensure intelligibility of the instructions,  
 274 only subjects from the United States who reported English as their first language were sampled.  
 275

## 276 2.4 PERFORMANCE EVALUATION

277  
 278 Given the subjective nature of the task (e.g., Are “balloons”, “flower bouquet”, or “ice cream”  
 279 all equally valid as an answer for the instructions in Figure 2?) and the potential for correct but  
 280 variable answers, we recruited 376 naïve subjects on Prolific to grade answers (LLM and human)  
 281 from the studies described above. Subjects were shown a label along with a corresponding image  
 282 approximating the final outcome of a set of instructions. They were asked to rate the reasonableness  
 283 of the label describing the image we created *in lieu* of target mental images. We collected 2030  
 284 unique answers from LLMs and humans in our mental imagery experiments. We excluded 122  
 285 of these answers because they were nonsensical, explicitly non-answers (e.g., “unsure”, “I don’t  
 286 know”; see Appendix E.2 for discussion), restatements of the instructions, or sexually explicit. We  
 287 ended with a final set of 1911 valid answers to use as labels. Each subject grader was given 30 of  
 288 these labels with the prompt: “How well does this image represent <label>?” and they were asked  
 289 to respond on with a 5-point scale: “Not at all”, “A little”, “Moderately”, “A lot”, “Completely”. In  
 290 addition, the authors provided independent “expert” evaluation of all of the labels. The final score  
 291 used to grade each valid response in our study was a weighted average of the expert’s grades and the  
 292 outsourced grades given by the Prolific subjects (see Appendix D.1).

## 293 3 RESULTS

### 294 3.1 HUMAN PERFORMANCE

295  
 296 Humans subjects exhibited an average performance of 54.7% (of the maximum possible score) in our  
 297 60-item task. We established that all of the 48 new instruction sets were doable (though the hardest  
 298 ones only received one or two meaningful answers from the entire subject population). Subjects  
 299 received close to perfect scores on the easiest instruction sets, with only one or two non-meaningful  
 300 answers. This offered us a good range of difficulties which was optimal for testing both human and  
 301 artificial model abilities. (See Appendix D.2 and Supplemental Figure S11 for more information on  
 302 item difficulty estimation and difficulty distribution).  
 303

304 When we looked exclusively at our 48 newly designed items, we observed a comparable perfor-  
 305 mance between our subjects’ performance and that of Finke et al.’s subjects in their original 12  
 306 items (52.6% and 56.1% of the maximum possible score, respectively).<sup>4</sup> Notably, our subjects’  
 307 performance on the 12 items following Finke et al.’s was higher (63%). This difference could po-  
 308 tentially owe to the fact that our set has a wider range of difficulty levels both in terms of number of  
 309 steps per trial and in terms of compositionality, complexity of transformations, and recognizability  
 310 of the final shape (all of which were explicitly desired traits in our experiment), or it could be simply  
 311 due to our rewritten instructions.

312 Finally, subjects’ VVIQ scores were well within expected bounds and we found a small negative  
 313 correlation between performance and mental imagery capacity VVIQ (see Appendix D.3 for further  
 314 discussion of VVIQ results).  
 315

### 316 3.2 RAPID ADVANCEMENT IN 2025

317 OpenAI’s o3 model family, as well as GPT-5, vastly outperformed every preexisting model, surpass-  
 318 ing the human baseline (humans were 9.4% below o3, which performed at 64.1%,  $\chi^2 = 28.631$ ,  
 319  $p < .00001$ ,  $CI = [-0.128, -0.06]$ ; humans vs o3-Pro: -11.9% difference,  $\chi^2 = 45.76$ ,  
 320  $p < .00001$ ,  $CI = [-0.153, -0.086]$ ; humans vs GPT-5: -12.3% difference, making GPT-5 the  
 321

322 <sup>4</sup>In Finke et al., each participant provided responses for six items. We normalized Finke et al.’s scores to  
 323 our scoring-system by assigning 5 points for each correct and 1 point for each incorrect answer to each label  
 (the minimum score in our paradigm)

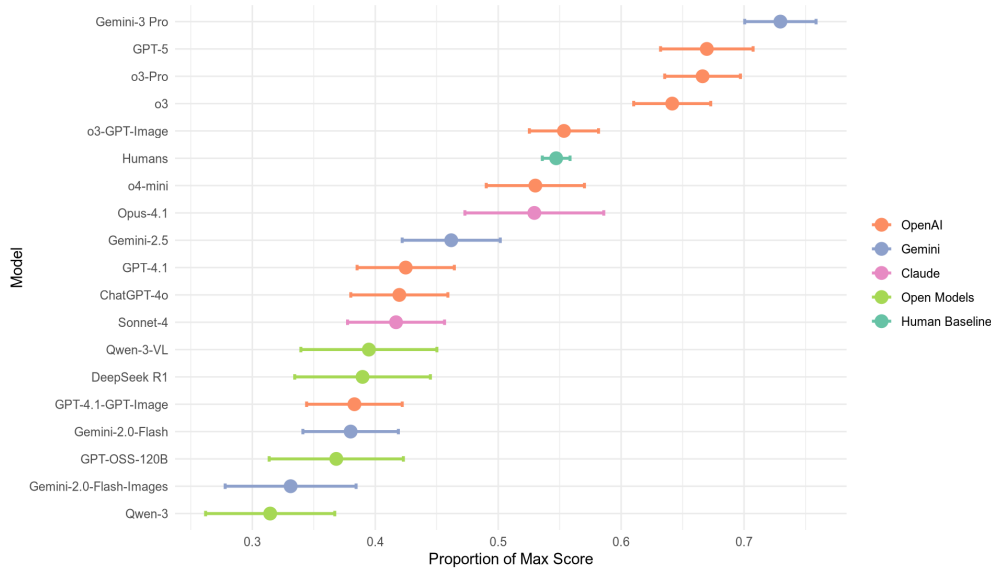


Figure 3: Performance results in humans and LLMs. Data shows proportion of maximum possible score for all tested models. Only Gemini 3 Pro, GPT-5, and the o3 family significantly surpass the human baseline. Error bars indicate 95% confidence intervals.

best model at 67%,  $\chi^2 = 33.302$ ,  $p < .00001$ ,  $CI = [-0.163, -0.082]$ ). Furthermore, Gemini 3 Pro reached a new frontier on our task: demolishing the human baseline by 18.2% (humans vs. Gemini 3 Pro:  $-18.2\%$  difference,  $\chi^2 = 108.103$ ,  $p < .00001$ ,  $CI = [-0.214, -0.151]$ ).<sup>5</sup> We show the stark gap between o3, GPT-5, Gemini 3 Pro, the human baseline, and every other model we tested in Figure 3. Based on our scoring methodology (Appendix D.1), we graded the outputs of each model (and the human baseline) and calculated the maximum possible score (see Table 1 for full scores; see Supplemental Table S5 for results of the 48-novel item subset and Supplemental Table S4 for results of the 12-items following Finke et al.).

The only other models to perform non-significantly different from the human baseline on our task were o4-mini ( $\chi^2 = 0.577$ ,  $p = .4477$ ,  $CI = [-0.025, 0.059]$ ) and Claude Opus 4.1 ( $\chi^2 = 0.299$ ,  $p = .5845$ ,  $CI = [-0.042, 0.077]$ ). Somewhat surprisingly, we found that adding images to o3 significantly decreased the model’s performance although it remained comparable to the human baseline (o3 vs. o3 with GPT-image-1: 8.8% difference,  $\chi^2 = 16.139$ ,  $p < .0001$ ,  $CI = [0.045, 0.131]$ , humans vs o3 with GPT-image-1:  $\chi^2 = 0.143$ ,  $p = .7057$ ,  $CI = [-0.037, 0.024]$ ). The older or cheaper models, however, performed very poorly across the board. We looked at two other models from OpenAI: ChatGPT-4o and GPT-4.1 (with and without images), both performed significantly worse than the o3 model family (see Appendix E.4.1). Claude Sonnet, Gemini 2.5 Pro, and Gemini 2.0 Flash all performed poorly. Gemini 2.0 Flash with images performed the worst of all proprietary models we tested.

Our testing of open models was extremely disappointing with all models performing worse than most, if not all, of the proprietary models. We discuss potential reasons for why this may be the case in Section 3.5.

Finally, we also measured the effect of the ‘reasoning\_effort’ parameter on the best performing OpenAI models. We found that higher reasoning effort led to improved results on our task (see Appendix E.1 and Supplemental Figures S4 and S5).

<sup>5</sup>Statistical significance in the main results presented in Figure 3 and Table 1 was determined after correcting for multiple comparisons using Bonferroni:  $\alpha = 0.05 / 18 = 0.0028$ .

Table 1: Human and LLMs scores

Agent	Score	Max Possible Score	Proportion
Humans	4098.217	7490	0.5472
o3***	577.390	900	0.6415
o3 + GPT-image-1 <sup>ns</sup>	664.182	1200	0.5535
o3-Pro***	599.621	900	0.6662
GPT-4.1	254.862	600	0.4248
GPT-4.1 + GPT-image-1	229.827	600	0.3830
o4-mini <sup>ns</sup>	318.131	600	0.5302
Gemini 2.5 Pro	227.074	600	0.4618
Gemini 2.0 Flash	227.982	600	0.3425
Gemini 2.0 Flash + Images	99.345	300	0.3800
Claude Sonnet 4	250.140	600	0.4169
Claude Opus 4.1 <sup>ns</sup>	158.819	300	0.5294
GPT-5***	401.883	600	0.6697
<b>Gemini 3 Pro***</b>	<b>656.589</b>	<b>900</b>	<b>0.7295</b>
DeepSeek R1	116.900	300	0.3897
Qwen 3	94.358	300	0.3145
Qwen 3 VL	118.442	300	0.3948
gpt-oss-120b	110.483	300	0.3682

Model in bold indicates highest performer in the group; the human baseline is in green; models in purple surpass the human baseline significantly [\*\*\*  $p < .001$ ]; models in blue are not significantly [<sup>ns</sup>] different from the human baseline and the rest in white are significantly lower [ $p < .001$ ]. Significance and non-significance determined after Bonferroni correction for multiple comparisons. See Appendix E.4.1

### 3.3 IMAGE-AIDED REASONING

Generating images, and solving the task using them, produced disappointing results. Perhaps unsurprisingly, in all cases of our image-aided paradigm the model performance dropped or, at best, stayed the same: o3 vs. o3 with GPT-image-1 (8.8% difference;  $\chi^2 = 16.139$ ,  $p < .0001$ ,  $CI = [0.045, 0.131]$ ); GPT-4.1 vs. GPT-4.1 with GPT-image-1 (4.2% difference;  $\chi^2 = 1.999$ ,  $p = .1574$ ,  $CI = [-0.015, 0.099]$ ); Gemini 2.0 Flash vs. Gemini 2.0 Flash with images (4.9% difference;  $\chi^2 = 1.854$ ,  $p = .1733$ ,  $CI = [-0.02, 0.117]$ ). We note, however, that o3’s strong performance allowed greater room for a significant decrease. It is unclear what the overall effect of image-aided reasoning is, as the models still found some success (though diminished), and more exploration of its effects is needed (Yang et al., 2025; Wu et al., 2024). Notably, modification of the ‘reasoning\_effort’ hyperparameter led to almost identical results, unlike what happened with the standard models without images (See Appendix E.1.)

### 3.4 MULTIPLE- VS. SINGLE-CONTEXT

We initially ran each model (excluding Gemini 2.0 Flash with images and o3 with images due to token limitations) in both a single context for all instructions as well as in a new context for each set of instructions (multiple-context). In our analysis of o3 and o3-Pro we found that including previous examples in context did not significantly change the overall performance (SC vs. MC in o3  $\chi^2 = 0.1064$ ,  $p = .7443$ ,  $CI = [-0.056, 0.083]$ ; and in o3-Pro  $\chi^2 = 0.02$ ,  $p = .887$ ,  $CI = [-0.061, 0.075]$ ). This indicates that in-context learning was not significantly beneficial for this task. Because of this, we did not differentiate between context types for statistical analysis and instead analyzed results from both types of context together. Additionally, when we further tested several additional models with different reasoning levels, we only tested them in multiple-context.

432 We graph the performance of the context interval variations of all tested models in Supplemental  
433 Figure S2.

### 435 3.5 OPEN MODEL FAILURE

436  
437 Across the board, the open models we tested performed horribly. Qwen 3 was the single worst  
438 performing model, and no open model met or surpassed the human baseline. We are not entirely  
439 sure as to the cause of this (due to not having access to architectural specifications of proprietary  
440 models), but, nevertheless, we were able to learn at least one somewhat interesting point.

441 Qwen 3 and Qwen 3 VL did not have a significant difference in performance (after accounting for  
442 multiple-comparisons). Qwen 3 vs. Qwen 3 VL:  $-8.03\%$  difference,  $\chi^2 = 3.88$ ,  $p = .0489$ ,  $CI =$   
443  $[-0.16, -0.001]$ . We found this notable due to the architecture of the model Bai et al. (2025); most  
444 critically, the vision-language alignment step. By aligning visual information to a text embedding,  
445 the model learns how to represent visual information textually (and therefore propositionally). The  
446 other open models did not include this step, and therefore, may have had reduced performance.

## 448 4 DISCUSSION

449  
450 Our results were surprising. LLMs successfully accomplished a task in which humans are believed  
451 to rely (almost) exclusively on visual mental imagery. They also offer an interesting window into  
452 the capacities of advanced artificial language systems to provide insight on tasks that are thought  
453 to require something beyond what language models are capable of. Gemini Pro 3, GPT-5 and the  
454 o3 Language Reasoning Model family outperformed humans across the board. These models do  
455 not have any (known, immediate) access to any form of image processing built-in by default when  
456 dealing with text decoding. Additionally, we can infer that no image generation was being used  
457 unless explicitly called upon due to the decreased cost of simple inference. Thus, these models  
458 should not have been able to complete our task so successfully given the dominant pictorial views  
459 on mental imagery. It would seem, however, that these LLMs completed our task via language token  
460 manipulations.

461 However, there is an alternative explanation, potentially orthogonal to the pictorial and propositional  
462 accounts. On this view, mental imagery is not a monolithic capacity; rather it must be distinguished  
463 into two capacities: spatial and object imagery (Phillips, 2025; Teng, 2025). According to this  
464 distinction, imagining objects and their surface features is supported by neural and psychological  
465 mechanisms that are different from the mechanisms supporting imagining the *spatial relations* be-  
466 tween objects. Evidence for this position comes from neurological patients with lesions resulting  
467 in preserved spatial reasoning abilities despite losing conscious mental imagery (Farah, 1988). It is  
468 also supported by behavioral work with aphantasics who exhibit normal results in spatial imagery  
469 questionnaires and (almost) normal performance in mental imagery tasks that rely heavily on spa-  
470 tial relations such as remembering a scene and mental rotation, which is clearly related to the task  
471 we used here (Bainbridge et al., 2021; Dawes et al., 2022). (See Appendix D.3 for discussion of  
472 aphantasic subjects in our sample.)

473 While LLMs' architecture, training, and data processing is primarily based on text, text-only mod-  
474 els can acquire representations of spatial concepts (Patel & Pavlick, 2022) and develop internal  
475 representations matching a spatial layout solely through procedural descriptions of moving through  
476 spaces. Moreover, embeddings from different modalities (e.g., vision and text) can be mapped to  
477 a shared representational space (Radford et al., 2021; Girdhar et al., 2023). It is thus possible that  
478 while relying solely on textual token manipulation, the most advanced LLMs are still able to extract  
479 the required spatial relations of the objects in each step of our instruction sets to perform at or above  
480 human level. This interpretation may help bridge different theories of mental imagery.

481 Notably, there is some probability of the original 12 items in the Finke et al. task being in the training  
482 data. This, however, cannot easily explain away our results. First, only 12 out of 60 instruction sets  
483 appeared in their original paper; the rest of them are completely novel designs. Second, the novel  
484 items include rather idiosyncratic examples that would be astounding if anything like them were  
485 explicitly in the training data (e.g., a computer mouse made with an S, a C, a horizontal line, and  
a D). Third, and related to the previous point, even if the *type* of task is present in the training  
data, and even if LLMs have information about the shape of letters (e.g., they know an 'o' is like

486 a circle and they know ice cream can be represented with circles), the models still have to solve  
487 a challenging compositional task: They need to put together all the elements, in the right spatial  
488 layout, in some cases after 4 transformations including rotation and mirroring, and only then use  
489 the resulting composite novel shape to “read out” the actual answer. This demanding task goes  
490 well beyond knowing that ice cream icons have circles (notoriously, an enormous amount of other  
491 things can also be drawn using circles). Fourth, no model, not even the best performing ones,  
492 universally solved all the original Finke items, suggesting that the models are not simply finding a  
493 ready-made solution from their training data. Finally, in the case of some models (e.g., GPT 4.1 and  
494 o3) we have reasons to believe that they may share their training data (both have a June 01, 2024  
495 knowledge cutoff). Even if some information relevant to our task were buried in the models’ training  
496 data, it is the parameters and general architecture of the models that ultimately determine how well  
497 they were able to find relevant information and solve our novel items. Thus, our data shows that  
498 some advanced LLMs can reason about composite shapes and their spatial layout by relying solely  
499 on linguistic embeddings in ways that seriously challenge the hypothesis that a pictorial format is  
500 necessary for completing our task.

501 Frontier LLMs give a new perspective to the debate on the formats of mental imagery, re-opening  
502 questions about the necessity of iconic mental imagery and the adequacy of classic tasks to test  
503 it. Furthermore, our results also open an important question in computer science about the kind of  
504 tasks that our most advanced language models can accomplish providing an opportunity to create  
505 new, complex benchmarks in sophisticated cognitive tasks.

## 506 507 508 5 CONCLUSIONS

509  
510  
511 Advancements in Large Reasoning Models have progressed so quickly that testing all their possible  
512 emergent properties poses serious challenges. Our research shows how to test one such property:  
513 propositional reasoning-based mental imagery. We determined that Gemini Pro 3, GPT-5 and the  
514 o3 family of models is more than capable of solving problems traditionally thought to require visual  
515 imagery. Furthermore, we note the difference in capabilities between OpenAI, Claude, and Gem-  
516 ini models in this form of advanced reasoning. Our instruction sets were created *ex novo*, so we  
517 can be confident that the performance we recorded is not an artifact of contaminated training data.  
518 Additionally, models did not universally succeed on the original items, which *could* exist within  
519 their training data. Our results could be deeply impactful, both for the artificial intelligence commu-  
520 nity, for examining and identifying a capability not yet measured within the most advanced models,  
521 and also for the cognitive science community, for discovering results that provide insight into the  
522 strategies and techniques used to accomplish imagery-dependent tasks. Through further analysis  
523 and experimentation on Large Language Reasoning Models, we may discover more about different  
524 ways in which the human mind can work (see Appendix F for Future Work).

## 525 526 527 6 LIMITATIONS

528  
529  
530 Due to the bespoke nature of our task, the amount of data collected is insufficient to make strong  
531 conclusions about similarly performing models (e.g., to differentiate between the performance of  
532 o3-Pro and GPT-5). Additionally, as o3 and GPT-image-1 are very compute-heavy models, data  
533 collection takes significant time and computational resources, which is an important consideration  
534 both from a practical and a theoretical standpoint when benchmarking. These characteristics of  
535 the models and of our task prevent significant iterations of data collection until models improve  
536 enough for this to be feasible. Notably, GPT-5 reaches similar performance to o3-Pro in significantly  
537 shorter time, though with more reasoning tokens, pointing to GPT-5’s higher processing efficiency.  
538 Similarly, even further advancement occurred with Gemini 3 Pro (faster and cheaper processing),  
539 despite it having the highest performance of all models. Finally, the state-of-the-art frontier models  
are all closed weight and closed architecture. We therefore cannot speculate about the underlying  
causes of our results or the difference in performance across models.

## 7 ETHICS STATEMENT

The experiments involving human participants were approved by the authors’ Institutional Review Board. All data provided by the authors’ that had any identifiable information has been removed. LLM usage related to this project is addressed in Appendix A.

## 8 REPRODUCIBILITY STATEMENT

In order to reproduce our results, we provide our experiment code and all data used in the production of this manuscript in Appendix B. We provide information on model selection and features in Table S1 and the exact versions of the models we used in Table S2. Furthermore, we provide information on the technical setup of our project in Appendix G, including information on our Python and R environments, exact model runs, hardware, and financial costs.

## REFERENCES

- Shuai Bai, Yuxuan Cai, Ruizhe Chen, Keqin Chen, Xionghui Chen, Zesen Cheng, Lianghao Deng, Wei Ding, Chang Gao, Chunjiang Ge, Wenbin Ge, Zhifang Guo, Qidong Huang, Jie Huang, Fei Huang, Binyuan Hui, Shutong Jiang, Zhaohai Li, Mingsheng Li, Mei Li, Kaixin Li, Zicheng Lin, Junyang Lin, Xuejing Liu, Jiawei Liu, Chenglong Liu, Yang Liu, Dayiheng Liu, Shixuan Liu, Dunjie Lu, Ruilin Luo, Chenxu Lv, Rui Men, Lingchen Meng, Xuancheng Ren, Xingzhang Ren, Sibao Song, Yuchong Sun, Jun Tang, Jianhong Tu, Jianqiang Wan, Peng Wang, Pengfei Wang, Qiuyue Wang, Yuxuan Wang, Tianbao Xie, Yiheng Xu, Haiyang Xu, Jin Xu, Zhibo Yang, Mingkun Yang, Jianxin Yang, An Yang, Bowen Yu, Fei Zhang, Hang Zhang, Xi Zhang, Bo Zheng, Huiyuan Zhong, Jingren Zhou, Fan Zhou, Jing Zhou, Yuanzhi Zhu, and Ke Zhu. Qwen3-vl technical report, 2025. URL <https://arxiv.org/abs/2511.21631>.
- Wilma A. Bainbridge, Zoë Pounder, Alison F. Eardley, and Chris I. Baker. Quantifying aphantasia through drawing: Those without visual imagery show deficits in object but not spatial memory. *Cortex*, 135:159–172, 2021. ISSN 0010-9452. doi: 10.1016/j.cortex.2020.11.014.
- Jan Betley, Xuchan Bao, Martín Soto, Anna Sztyber-Betley, James Chua, and Owain Evans. Tell me about yourself: LLMs are aware of their learned behaviors, 2025. URL <https://arxiv.org/abs/2501.11120>.
- Eric J. Bigelow, John P. McCoy, and Tomer D. Ullman. Non-commitment in mental imagery. *Cognition*, 238:105498, 2023.
- Ned Block. *The Border between Seeing and Thinking*. Oxford University Press, 2023.
- Andrea Blomkvist. Aphantasia: In search of a theory. *Mind & Language*, 38(3):866–888, 2023. doi: <https://doi.org/10.1111/mila.12432>. URL <https://onlinelibrary.wiley.com/doi/abs/10.1111/mila.12432>.
- Alessia Bocchi, Marika Carrieri, Stefania Lancia, Valentina Quaresima, and Laura Piccardi. The key of the maze: The role of mental imagery and cognitive flexibility in navigational planning. *Neuroscience Letters*, 651:146–150, 2017. ISSN 0304-3940. doi: <https://doi.org/10.1016/j.neulet.2017.05.009>. URL <https://www.sciencedirect.com/science/article/pii/S0304394017303877>.
- Faeze Brahman, Sachin Kumar, Vidhisha Balachandran, Pradeep Dasigi, Valentina Pyatkin, Abhilasha Ravichander, Sarah Wiegrefe, Nouha Dziri, Khyathi Chandu, Jack Hessel, Yulia Tsvetkov, Noah A. Smith, Yejin Choi, and Hannaneh Hajishirzi. The art of saying no: Contextual noncompliance in language models. In A. Globerson, L. Mackey, D. Belgrave, A. Fan, U. Paquet, J. Tomczak, and C. Zhang (eds.), *Advances in Neural Information Processing Systems*, volume 37, pp. 49706–49748. Curran Associates, Inc., 2024. URL [https://proceedings.neurips.cc/paper\\_files/paper/2024/file/58e79894267cf72c66202228ad9c6057-Paper-Datasets\\_and\\_Benchmarks\\_Track.pdf](https://proceedings.neurips.cc/paper_files/paper/2024/file/58e79894267cf72c66202228ad9c6057-Paper-Datasets_and_Benchmarks_Track.pdf).

- 594 Patrick Byrne, Suzanna Becker, and Neil Burgess. Remembering the past and imagining the future:  
595 a neural model of spatial memory and imagery. *Psychological review*, 114(2):340, 2007.  
596
- 597 Zirui Chen and Michael F. Bonner. Universal dimensions of visual representation. *Science Advances*,  
598 11(27):eadw7697, 2025. doi: 10.1126/sciadv.adw7697. URL <https://www.science.org/doi/abs/10.1126/sciadv.adw7697>.  
599
- 600 Francois Chollet, Mike Knoop, Gregory Kamradt, and Bryan Landers. Arc prize 2024: Technical  
601 report, 2025. URL <https://arxiv.org/abs/2412.04604>.  
602
- 603 C.J. Dance, A. Ipser, and J. Simner. The prevalence of aphantasia (imagery weakness) in  
604 the general population. *Consciousness and Cognition*, 97:103243, 2022. ISSN 1053-8100.  
605 doi: <https://doi.org/10.1016/j.concog.2021.103243>. URL <https://www.sciencedirect.com/science/article/pii/S1053810021001690>.  
606
- 607 Alexei J. Dawes, Rebecca Keogh, Sarah Robuck, and Joel Pearson. Memories with a blind mind:  
608 Remembering the past and imagining the future with aphantasia. *Cognition*, 227:105192, 2022.  
609 ISSN 0010-0277. doi: 10.1016/j.cognition.2022.105192.  
610
- 611 Dorottya Demszky, Diyi Yang, David S Yeager, Christopher J Bryan, Margaret Clapper, Susannah  
612 Chandhok, Johannes C Eichstaedt, Cameron Hecht, Jeremy Jamieson, Meghann Johnson, et al.  
613 Using large language models in psychology. *Nature Reviews Psychology*, 2(11):688–701, 2023.  
614
- 615 Nadine Dijkstra, Sander E Bosch, and Marcel AJ van Gerven. Shared neural mechanisms of visual  
616 perception and imagery. *Trends in cognitive sciences*, 23(5):423–434, 2019.
- 617 Qingxiu Dong, Lei Li, Damai Dai, Ce Zheng, Jingyuan Ma, Rui Li, Heming Xia, Jingjing Xu,  
618 Zhiyong Wu, Tianyu Liu, Baobao Chang, Xu Sun, Lei Li, and Zhifang Sui. A survey on in-  
619 context learning, 2024. URL <https://arxiv.org/abs/2301.00234>.  
620
- 621 Martha J Farah. Is visual imagery really visual? overlooked evidence from neuropsychology. *Psy-*  
622 *chological review*, 95(3):307, 1988.  
623
- 624 Jeanne Farrington. Seven plus or minus two. *Performance Improvement Quarterly*, 23(4):113–116,  
625 2011. doi: <https://doi.org/10.1002/piq.20099>. URL <https://onlinelibrary.wiley.com/doi/abs/10.1002/piq.20099>.  
626
- 627 Bill Faw. Conflicting intuitions may be based on differing abilities: Evidence from mental imaging  
628 research. *Journal of Consciousness Studies*, 16:45–68, 01 2009.  
629
- 630 Ronald Finke. *Creative Imagery: Discoveries and Inventions in Visualization*. Psychology Press,  
631 1990.
- 632 Ronald A Finke, Steven Pinker, and Martha J Farah. Reinterpreting visual patterns in mental im-  
633 agery. *Cognitive Science*, 13(1):51–78, 1989.  
634
- 635 Michael C. Frank and Noah D. Goodman. Cognitive modeling using artificial intelligence.  
636 *Annual Review of Psychology*, 2025. ISSN 0066-4308. doi: <https://doi.org/10.1146/annurev-psych-030625-040748>. URL <https://www.annualreviews.org/content/journals/10.1146/annurev-psych-030625-040748>.  
637  
638
- 639 Rohit Girdhar, Alaaeldin El-Nouby, Zhuang Liu, Mannat Singh, Kalyan Vasudev Alwala, Armand  
640 Joulin, and Ishan Misra. ImageBind: One embedding space to bind them all. *arXiv*, 2023. doi:  
641 10.48550/arxiv.2305.05665.  
642
- 643 Dan Hendrycks, Collin Burns, Steven Basart, Andy Zou, Mantas Mazeika, Dawn Song, and Ja-  
644 cob Steinhardt. Measuring massive multitask language understanding, 2021. URL <https://arxiv.org/abs/2009.03300>.  
645
- 646 Emily A Holmes and Andrew Mathews. Mental imagery in emotion and emotional disorders. *Clin-*  
647 *ical psychology review*, 30(3):349–362, 2010.

- 648 Kaiyi Huang, Kaiyue Sun, Enze Xie, Zhenguo Li, and Xihui Liu. T2i-compbench: A com-  
649 prehensive benchmark for open-world compositional text-to-image generation. In A. Oh,  
650 T. Naumann, A. Globerson, K. Saenko, M. Hardt, and S. Levine (eds.), *Advances in Neural*  
651 *Information Processing Systems*, volume 36, pp. 78723–78747. Curran Associates, Inc., 2023.  
652 URL [https://proceedings.neurips.cc/paper\\_files/paper/2023/file/  
653 f8ad010cdd9143dbb0e9308c093aff24-Paper-Datasets\\_and\\_Benchmarks.  
654 pdf](https://proceedings.neurips.cc/paper_files/paper/2023/file/f8ad010cdd9143dbb0e9308c093aff24-Paper-Datasets_and_Benchmarks.pdf).
- 655 Anna A. Ivanova, Aalok Sathe, Benjamin Lipkin, Unnathi Kumar, Setayesh Radkani, Thomas H.  
656 Clark, Carina Kauf, Jennifer Hu, R. T. Pramod, Gabriel Grand, Vivian Paulun, Maria Ryskina,  
657 Ekin Akyürek, Ethan Wilcox, Nafisa Rashid, Leshem Choshen, Roger Levy, Evelina Fedorenko,  
658 Joshua Tenenbaum, and Jacob Andreas. Elements of world knowledge (ewok): A cognition-  
659 inspired framework for evaluating basic world knowledge in language models, 2025. URL  
660 <https://arxiv.org/abs/2405.09605>.
- 661 Saurav Kadavath, Tom Conerly, Amanda Askell, Tom Henighan, Dawn Drain, Ethan Perez,  
662 Nicholas Schiefer, Zac Hatfield-Dodds, Nova DasSarma, Eli Tran-Johnson, Scott Johnston, Sheer  
663 El-Showk, Andy Jones, Nelson Elhage, Tristan Hume, Anna Chen, Yuntao Bai, Sam Bow-  
664 man, Stanislav Fort, Deep Ganguli, Danny Hernandez, Josh Jacobson, Jackson Kernion, Shauna  
665 Kravec, Liane Lovitt, Kamal Ndousse, Catherine Olsson, Sam Ringer, Dario Amodei, Tom  
666 Brown, Jack Clark, Nicholas Joseph, Ben Mann, Sam McCandlish, Chris Olah, and Jared Ka-  
667 plan. Language models (mostly) know what they know, 2022. URL [https://arxiv.org/  
668 abs/2207.05221](https://arxiv.org/abs/2207.05221).
- 669 Lachlan Kay, Rebecca Keogh, and Joel Pearson. Slower but more accurate mental rota-  
670 tion performance in aphantasia linked to differences in cognitive strategies. *Consciousness*  
671 *and Cognition*, 121:103694, 2024. ISSN 1053-8100. doi: [https://doi.org/10.1016/j.concog.  
672 2024.103694](https://doi.org/10.1016/j.concog.2024.103694). URL [https://www.sciencedirect.com/science/article/pii/  
673 S1053810024000618](https://www.sciencedirect.com/science/article/pii/S1053810024000618).
- 674 Rebecca Keogh, Marcus Wicken, and Joel Pearson. Visual working memory in aphantasia: Retained  
675 accuracy and capacity with a different strategy. *Cortex*, 143:237–253, 2021. ISSN 0010-9452.  
676 doi: <https://doi.org/10.1016/j.cortex.2021.07.012>. URL [https://www.sciencedirect.  
677 com/science/article/pii/S0010945221002628](https://www.sciencedirect.com/science/article/pii/S0010945221002628).
- 678 Mohammad Abdullah Matin Khan, M Saiful Bari, Xuan Long Do, Weishi Wang, Md Rizwan  
679 Parvez, and Shafiq Joty. xcodeeval: A large scale multilingual multitask benchmark for code  
680 understanding, generation, translation and retrieval, 2023. URL [https://arxiv.org/abs/  
681 2303.03004](https://arxiv.org/abs/2303.03004).
- 682 Douwe Kiela and Léon Bottou. Learning image embeddings using convolutional neural networks  
683 for improved multi-modal semantics. In Alessandro Moschitti, Bo Pang, and Walter Daelemans  
684 (eds.), *Proceedings of the 2014 Conference on Empirical Methods in Natural Language Process-*  
685 *ing (EMNLP)*, pp. 36–45, Doha, Qatar, October 2014. Association for Computational Linguistics.  
686 doi: 10.3115/v1/D14-1005. URL <https://aclanthology.org/D14-1005/>.
- 687 Donghyun Kim, Kuniaki Saito, Kate Saenko, Stan Sclaroff, and Bryan Plummer. Mule: Multimodal  
688 universal language embedding. *Proceedings of the AAAI Conference on Artificial Intelligence*, 34  
689 (07):11254–11261, Apr. 2020. doi: 10.1609/aaai.v34i07.6785. URL [https://ojs.aaai.  
690 org/index.php/AAAI/article/view/6785](https://ojs.aaai.org/index.php/AAAI/article/view/6785).
- 691 Najoung Kim and Tal Linzen. COGS: A compositional generalization challenge based on se-  
692 mantic interpretation. In Bonnie Webber, Trevor Cohn, Yulan He, and Yang Liu (eds.),  
693 *Proceedings of the 2020 Conference on Empirical Methods in Natural Language Processing*  
694 *(EMNLP)*, pp. 9087–9105, Online, November 2020. Association for Computational Linguis-  
695 tics. doi: 10.18653/v1/2020.emnlp-main.731. URL [https://aclanthology.org/2020.  
696 emnlp-main.731/](https://aclanthology.org/2020.emnlp-main.731/).
- 697 Tomáš Kočiský, Jonathan Schwarz, Phil Blunsom, Chris Dyer, Karl Moritz Hermann, Gábor Melis,  
698 and Edward Grefenstette. The NarrativeQA reading comprehension challenge. *Transactions of*  
699 *the Association for Computational Linguistics*, 6:317–328, 2018. doi: 10.1162/tacl.a.00023.  
700 URL <https://aclanthology.org/Q18-1023/>.
- 701

- 702 Stephen M Kosslyn. *Image and brain: The resolution of the imagery debate*. MIT Press, 1996.  
703
- 704 Stephen Michael Kosslyn. Scanning visual images: Some structural implications. *Perception &*  
705 *Psychophysics*, 14(1):90–94, 1973.
- 706 Kristina Krasich, Kevin O’Neill, and Felipe De Brigard. Looking at mental images: Eye-tracking  
707 mental simulation during retrospective causal judgment. *Cognitive Science*, 48(3):e13426, 2024.  
708 doi: <https://doi.org/10.1111/cogs.13426>. URL <https://onlinelibrary.wiley.com/doi/abs/10.1111/cogs.13426>.
- 710 AJ Larner, AP Leff, and PC Nachev. Phantasia, aphantasia, and hyperphantasia: Empirical data  
711 and conceptual considerations. *Neuroscience & Biobehavioral Reviews*, 164:105819, 2024.  
712 ISSN 0149-7634. doi: <https://doi.org/10.1016/j.neubiorev.2024.105819>. URL <https://www.sciencedirect.com/science/article/pii/S0149763424002884>.
- 714 Alex Lawsen. Comment on the illusion of thinking: Understanding the strengths and limitations  
715 of reasoning models via the lens of problem complexity, 2025. URL <https://arxiv.org/abs/2506.09250>.
- 718 Florent Lebon. Revisiting the mental imagery debate: New evidence from aphantasia and neu-  
719 roimaging, Sep 2025. URL [osf.io/preprints/psyarxiv/cfh85\\_v1](https://osf.io/preprints/psyarxiv/cfh85_v1).
- 720 Anna Leshinskaya, Taylor Webb, Ellie Pavlick, Jiahai Feng, Gustaw Opielka, Claire Stevenson, and  
721 Idan A Blank. Cognitively inspired interpretability in large neural networks. In *Proceedings of*  
722 *the Annual Meeting of the Cognitive Science Society*, volume 47, 2025.
- 724 Yuan Li, Yue Huang, Hongyi Wang, Xiangliang Zhang, James Zou, and Lichao Sun. Quantifying  
725 ai psychology: A psychometrics benchmark for large language models, 2024. URL <https://arxiv.org/abs/2406.17675>.
- 727 Nan Liu, Shuang Li, Yilun Du, Antonio Torralba, and Joshua B. Tenenbaum. Compositional vi-  
728 sual generation with composable diffusion models. In Shai Avidan, Gabriel Brostow, Moustapha  
729 Cissé, Giovanni Maria Farinella, and Tal Hassner (eds.), *Computer Vision – ECCV 2022*, pp.  
730 423–439, Cham, 2022. Springer Nature Switzerland. ISBN 978-3-031-19790-1.
- 732 Ryan Liu, Jiayi Geng, Addison J. Wu, Ilia Sucholutsky, Tania Lombrozo, and Thomas L. Griffiths.  
733 Mind your step (by step): Chain-of-thought can reduce performance on tasks where thinking  
734 makes humans worse, 2025. URL <https://arxiv.org/abs/2410.21333>.
- 736 Tania Lombrozo. Learning by thinking in natural and artificial minds. *Trends in Cognitive Sciences*,  
737 28:1011–1022, 2024.
- 738 Joel J. Lorenzatti. Aphantasia: a philosophical approach. *Philosophical Psychology*, 38(4):1476–  
739 1504, 2025. doi: [10.1080/09515089.2023.2253854](https://doi.org/10.1080/09515089.2023.2253854). URL <https://doi.org/10.1080/09515089.2023.2253854>.
- 741 Andrey Malinin and Mark Gales. Uncertainty estimation in autoregressive structured prediction,  
742 2021. URL <https://arxiv.org/abs/2002.07650>.
- 743 David F. Marks. Visual imagery differences in the recall of pictures. *British Journal*  
744 *of Psychology*, 64(1):17–24, 1973. doi: <https://doi.org/10.1111/j.2044-8295.1973.tb01322.x>.  
745 x. URL [https://bpspsychub.onlinelibrary.wiley.com/doi/abs/10.1111/](https://bpspsychub.onlinelibrary.wiley.com/doi/abs/10.1111/j.2044-8295.1973.tb01322.x)  
746 [j.2044-8295.1973.tb01322.x](https://bpspsychub.onlinelibrary.wiley.com/doi/abs/10.1111/j.2044-8295.1973.tb01322.x).
- 748 R. Thomas McCoy, Tal Linzen, Ewan Dunbar, and Paul Smolensky. Rnns implicitly implement  
749 tensor product representations, 2019. URL <https://arxiv.org/abs/1812.08718>.
- 750 Sam Whitman McGrath, Jacob Russin, Ellie Pavlick, and Roman Feiman. How can deep neural  
751 networks inform theory in psychological science? *Current Directions in Psychological Science*,  
752 33(5):325–333, 2024. doi: [10.1177/09637214241268098](https://doi.org/10.1177/09637214241268098). URL <https://doi.org/10.1177/09637214241268098>.
- 754 Matthias Michel, Jorge Morales, Ned Block, and Hakwan Lau. Aphantasia as imagery blindsight.  
755 *Trends in Cognitive Sciences*, 29(1):8–9, 2025. doi: [10.1016/j.tics.2024.11.002](https://doi.org/10.1016/j.tics.2024.11.002).

- 756 George A. Miller. The magical number seven, plus or minus two: Some limits on our capacity for  
757 processing information. *Psychological Review*, 63(2):81–97, 1956. doi: 10.1037/h0043158.  
758
- 759 Bence Nanay. Unconscious mental imagery. *Philosophical Transactions of the Royal Society B:*  
760 *Biological Sciences*, 376(1817):20190689, 2021. doi: 10.1098/rstb.2019.0689. URL <https://royalsocietypublishing.org/doi/abs/10.1098/rstb.2019.0689>.  
761
- 762 Thomas Naselaris, Cheryl A. Olman, Dustin E. Stansbury, Kamil Ugurbil, and Jack L. Gallant. A  
763 voxel-wise encoding model for early visual areas decodes mental images of remembered scenes.  
764 *NeuroImage*, 105:215–228, 2015. ISSN 1053-8119. doi: [https://doi.org/10.1016/j.neuroimage.](https://doi.org/10.1016/j.neuroimage.2014.10.018)  
765 2014.10.018. URL <https://www.sciencedirect.com/science/article/pii/S1053811914008428>.  
766
- 767 Richard E. Nisbett and Timothy D. Wilson. Telling more than we can know: Verbal reports on mental  
768 processes. *Psychological Review*, 84(3):231–259, 1977. doi: doi:10.1037/0033-295X.84.3.231.  
769
- 770 Daniela J Palombo, Signy Sheldon, and Brian Levine. Individual differences in autobiographical  
771 memory. *Trends in Cognitive Sciences*, 22(7):583–597, 2018.  
772
- 773 Roma Patel and Ellie Pavlick. Mapping language models to grounded conceptual spaces. In *Internat-*  
774 *ional Conference on Learning Representations*, 2022. URL [https://openreview.net/](https://openreview.net/pdf?id=gJcEM8sxHK)  
775 [pdf?id=gJcEM8sxHK](https://openreview.net/pdf?id=gJcEM8sxHK).
- 776 Ellie Pavlick. Symbols and grounding in large language models. *Philosophical Transactions of*  
777 *the Royal Society A: Mathematical, Physical and Engineering Sciences*, 381(2251):20220041,  
778 2023. doi: 10.1098/rsta.2022.0041. URL [https://royalsocietypublishing.org/](https://royalsocietypublishing.org/doi/abs/10.1098/rsta.2022.0041)  
779 [doi/abs/10.1098/rsta.2022.0041](https://royalsocietypublishing.org/doi/abs/10.1098/rsta.2022.0041).
- 780 Joel Pearson and Stephen M. Kosslyn. The heterogeneity of mental representation: Ending the im-  
781 agery debate. *Proceedings of the National Academy of Sciences*, 112(33):10089–10092, 2015.  
782 doi: 10.1073/pnas.1504933112. URL [https://www.pnas.org/doi/abs/10.1073/](https://www.pnas.org/doi/abs/10.1073/pnas.1504933112)  
783 [pnas.1504933112](https://www.pnas.org/doi/abs/10.1073/pnas.1504933112).  
784
- 785 Joel Pearson, Thomas Naselaris, Emily A Holmes, and Stephen M Kosslyn. Mental imagery: func-  
786 tional mechanisms and clinical applications. *Trends in cognitive sciences*, 19(10):590–602, 2015.  
787
- 788 Ian B. Phillips. Aphantasia reimaged. *Noûs*, pp. 1–25, 2025. doi: 10.1111/nous.12551.
- 789 Steven T Piantadosi, Dyana CY Muller, Joshua S Rule, Karthikeya Kaushik, Mark Gorenstein,  
790 Elena R Leib, and Emily Sanford. Why concepts are (probably) vectors. *Trends in Cognitive*  
791 *Sciences*, 28(9):844–856, 2024.
- 792 Dillon Plunkett, Adam Morris, Keerthi Reddy, and Jorge Morales. Self-interpretability: Llms can  
793 describe complex internal processes that drive their decisions, and improve with training, 2025.  
794 URL <https://arxiv.org/abs/2505.17120>.  
795
- 796 Zoë Pounder, Jane Jacob, Samuel Evans, Catherine Loveday, Alison F. Eardley, and Juha Silvanto.  
797 Only minimal differences between individuals with congenital aphantasia and those with typical  
798 imagery on neuropsychological tasks that involve imagery. *Cortex*, 148:180–192, 2022. doi:  
799 10.1037/h0043158.
- 800 Ofir Press, Muru Zhang, Sewon Min, Ludwig Schmidt, Noah A. Smith, and Mike Lewis. Measuring  
801 and narrowing the compositionality gap in language models, 2023. URL [https://arxiv.](https://arxiv.org/abs/2210.03350)  
802 [org/abs/2210.03350](https://arxiv.org/abs/2210.03350).
- 803 Zenon W Pylyshyn. What the mind’s eye tells the mind’s brain: A critique of mental imagery.  
804 *Psychological bulletin*, 80(1):1, 1973.  
805
- 806 Zenon W. Pylyshyn. Mental imagery: In search of a theory. *Behavioral and Brain Sciences*, 25(2):  
807 157–182, 2002. doi: 10.1017/S0140525X02000043.
- 808 Jake Quilty-Dunn. Is Iconic Memory Iconic? *Philosophy and Phenomenological Research*, 59  
809 (175):171 – 23, 07 2019. doi: 10.1111/phpr.12625. URL <https://www.dropbox.com/>.

- 810 Alec Radford, Jong Wook Kim, Chris Hallacy, Aditya Ramesh, Gabriel Goh, Sandhini Agar-  
811 wal, Girish Sastry, Amanda Askell, Pamela Mishkin, Jack Clark, Gretchen Krueger, and Ilya  
812 Sutskever. Learning transferable visual models from natural language supervision, 2021. URL  
813 <https://arxiv.org/abs/2103.00020>.
- 814
- 815 Santhosh Kumar Ramakrishnan, Erik Wijmans, Philipp Kraehenbuehl, and Vladlen Koltun. Does  
816 spatial cognition emerge in frontier models?, 2025. URL [https://arxiv.org/abs/2410.](https://arxiv.org/abs/2410.06468)  
817 06468.
- 818
- 819 David Rein, Betty Li Hou, Asa Cooper Stickland, Jackson Petty, Richard Yuanzhe Pang, Julien  
820 Dirani, Julian Michael, and Samuel R. Bowman. Gpqa: A graduate-level google-proof q&a  
821 benchmark, 2023. URL <https://arxiv.org/abs/2311.12022>.
- 822
- 823 Matthew Renze and Erhan Guven. The effect of sampling temperature on problem solving in large  
824 language models. In Yaser Al-Onaizan, Mohit Bansal, and Yun-Nung Chen (eds.), *Findings of*  
825 *the Association for Computational Linguistics: EMNLP 2024*, pp. 7346–7356, Miami, Florida,  
826 USA, November 2024. Association for Computational Linguistics. doi: 10.18653/v1/2024.  
827 findings-emnlp.432. URL [https://aclanthology.org/2024.findings-emnlp.](https://aclanthology.org/2024.findings-emnlp.432/)  
828 432/.
- 829
- 830 Oscar Sainz, Jon Ander Campos, Iker García-Ferrero, Julen Etxaniz, Oier Lopez de Lacalle, and  
831 Eneko Agirre. Nlp evaluation in trouble: On the need to measure llm data contamination for each  
832 benchmark, 2023. URL <https://arxiv.org/abs/2310.18018>.
- 833
- 834 Roger N. Shepard and Jacqueline Metzler. Mental rotation of three-dimensional objects. *Sci-*  
835 *ence*, 171(3972):701–703, 1971. doi: 10.1126/science.171.3972.701. URL [https://www.](https://www.science.org/doi/abs/10.1126/science.171.3972.701)  
836 [science.org/doi/abs/10.1126/science.171.3972.701](https://www.science.org/doi/abs/10.1126/science.171.3972.701).
- 837
- 838 Richard Shiffrin and Melanie Mitchell. Probing the psychology of ai models. *Proceedings of the*  
839 *National Academy of Sciences*, 120(10):e2300963120, 2023. doi: 10.1073/pnas.2300963120.  
840 URL <https://www.pnas.org/doi/abs/10.1073/pnas.2300963120>.
- 841
- 842 Parshin Shojaee, Iman Mirzadeh, Keivan Alizadeh, Maxwell Horton, Samy Bengio, and Mehrdad  
843 Farajtabar. The illusion of thinking: Understanding the strengths and limitations of reasoning  
844 models via the lens of problem complexity, 2025. URL [https://arxiv.org/abs/2506.](https://arxiv.org/abs/2506.06941)  
845 06941.
- 846
- 847 Lu Teng. Conscious schematic imagery in aphantasia. Unpublished manuscript, 2025.
- 848
- 849 Alan M Turing. I.—computing machinery and intelligence. *Mind.*, 59(236), 1950. ISSN 0026-4423.
- 850
- 851 Yiming Wang, Ziyang Zhang, Hanwei Chen, and Huayi Shen. Reasoning with large language mod-  
852 els on graph tasks: The influence of temperature. In *2024 5th International Conference on Com-*  
853 *puter Engineering and Application (ICCEA)*, pp. 630–634, 2024a. doi: 10.1109/ICCEA62105.  
854 2024.10603677.
- 855
- 856 Yubo Wang, Xueguang Ma, Ge Zhang, Yuansheng Ni, Abhranil Chandra, Shiguang Guo,  
857 Weiming Ren, Aaran Arulraj, Xuan He, Ziyang Jiang, Tianle Li, Max Ku, Kai Wang,  
858 Alex Zhuang, Rongqi Fan, Xiang Yue, and Wenhui Chen. Mmlu-pro: A more robust and  
859 challenging multi-task language understanding benchmark. In A. Globerson, L. Mackey,  
860 D. Belgrave, A. Fan, U. Paquet, J. Tomczak, and C. Zhang (eds.), *Advances in Neural Infor-*  
861 *mation Processing Systems*, volume 37, pp. 95266–95290. Curran Associates, Inc., 2024b.  
862 URL [https://proceedings.neurips.cc/paper\\_files/paper/2024/file/](https://proceedings.neurips.cc/paper_files/paper/2024/file/ad236edc564f3e3156e1b2feafb99a24-Paper-Datasets_and_Benchmarks_Track.pdf)  
863 [ad236edc564f3e3156e1b2feafb99a24-Paper-Datasets\\_and\\_Benchmarks\\_](https://proceedings.neurips.cc/paper_files/paper/2024/file/ad236edc564f3e3156e1b2feafb99a24-Paper-Datasets_and_Benchmarks_Track.pdf)  
Track.pdf.
- 864
- 865 Mark E. Wheeler, Steven E. Petersen, and Randy L. Buckner. Memory’s echo: Vivid remembering  
866 reactivates sensory-specific cortex. *Proceedings of the National Academy of Sciences*, 97(20):  
867 11125–11129, 2000. doi: 10.1073/pnas.97.20.11125. URL [https://www.pnas.org/doi/](https://www.pnas.org/doi/abs/10.1073/pnas.97.20.11125)  
868 [abs/10.1073/pnas.97.20.11125](https://www.pnas.org/doi/abs/10.1073/pnas.97.20.11125).

- 864 David J. Wright, Matthew W. Scott, Sarah N. Krautner, Pamela Barhoun, Maurizio Bertollo,  
865 Mark J. Campbell, Baptiste M. Waltzing, Stephan F. Dahm, Maaïke Esselaar, Cornelia Frank,  
866 Robert M. Hardwick, Ian Fuelscher, Ben Marshall, Nicola J. Hodges, Christian Hyde, and  
867 Paul S. Holmes. An international estimate of the prevalence of differing visual imagery abilities.  
868 *Frontiers in Psychology*, Volume 15 - 2024, 2024. ISSN 1664-1078. doi: 10.3389/fpsyg.  
869 2024.1454107. URL [https://www.frontiersin.org/journals/psychology/  
870 articles/10.3389/fpsyg.2024.1454107](https://www.frontiersin.org/journals/psychology/articles/10.3389/fpsyg.2024.1454107).
- 871 Wenshan Wu, Shaoguang Mao, Yadong Zhang, Yan Xia, Li Dong, Lei Cui, and  
872 Furu Wei. Mind's eye of llms: Visualization-of-thought elicits spatial reasoning in  
873 large language models. In A. Globerson, L. Mackey, D. Belgrave, A. Fan, U. Pa-  
874 quet, J. Tomczak, and C. Zhang (eds.), *Advances in Neural Information Process-  
875 ing Systems*, volume 37, pp. 90277–90317. Curran Associates, Inc., 2024. URL  
876 [https://proceedings.neurips.cc/paper\\_files/paper/2024/file/  
877 a45296e83b19f656392e0130d9e53cb1-Paper-Conference.pdf](https://proceedings.neurips.cc/paper_files/paper/2024/file/a45296e83b19f656392e0130d9e53cb1-Paper-Conference.pdf).
- 878 Daniel Wurgaft, Ekdeep Singh Lubana, Core Francisco Park, Hidenori Tanaka, Gautam Reddy,  
879 and Noah D. Goodman. In-context learning strategies emerge rationally, 2025. URL <https://arxiv.org/abs/2506.17859>.
- 880  
881 Daniel L. K. Yamins, Ha Hong, Charles F. Cadieu, Ethan A. Solomon, Darren Seibert, and James J.  
882 DiCarlo. Performance-optimized hierarchical models predict neural responses in higher visual  
883 cortex. *Proceedings of the National Academy of Sciences*, 111(23):8619–8624, 2014. doi:  
884 10.1073/pnas.1403112111. URL [https://www.pnas.org/doi/abs/10.1073/pnas.  
885 1403112111](https://www.pnas.org/doi/abs/10.1073/pnas.1403112111).
- 886  
887 Zeyuan Yang, Xueyang Yu, Delin Chen, Maohao Shen, and Chuang Gan. Machine mental imagery:  
888 Empower multimodal reasoning with latent visual tokens, 2025. URL [https://arxiv.org/  
889 abs/2506.17218](https://arxiv.org/abs/2506.17218).
- 890  
891 Adam Zeman. Aphantasia and hyperphantasia: exploring imagery vividness extremes. *Trends in  
892 Cognitive Sciences*, 28(5):467–480, 2024.
- 893  
894 Adam Zeman, Michaela Dewar, and Sergio Della Sala. Lives without imagery – congenital aphan-  
895 tasia. *Cortex*, 73:378–380, 2015. ISSN 0010-9452. doi: [https://doi.org/10.1016/j.cortex.  
896 2015.05.019](https://doi.org/10.1016/j.cortex.2015.05.019). URL [https://www.sciencedirect.com/science/article/pii/  
897 S0010945215001781](https://www.sciencedirect.com/science/article/pii/S0010945215001781).
- 898  
899  
900  
901  
902  
903  
904  
905  
906  
907  
908  
909  
910  
911  
912  
913  
914  
915  
916  
917

## A USAGE OF LARGE LANGUAGE MODELS

Outside of the usage as described in the rest of this paper, LLMs were used to generate code and documentation for running the experiments and statistical analyses. All code was manually checked and verified post-generation to ensure soundness.

In order to ensure prevention of data contamination: other than in testing, no LLM was given access to the instructions or any other data that may allow improved performance on the task. Additionally, we disabled sharing input and output data with the parent company of each model we used in our experiment whenever possible.

## B ACCESS TO CODE AND DATA

Our code and data is accessible under MIT License in our anonymous GitHub repository ([https://anonymous.4open.science/r/artificial\\_phantasia-825C/](https://anonymous.4open.science/r/artificial_phantasia-825C/)). All human subject data has been de-identified. Please refer to the README.md file in the repository for usage and explanatory information regarding the repository.

We provide code to run the experiment, view and re-perform our data analysis, and generate surveys for Qualtrics XM. Our dataset includes the instructions used for our task (along with the intended canonical form), the de-identified data from both humans and LLMs, the de-identified response ranking data, and the image representations of each intended image (the images from Finke et al., 1989 are their original versions for replicability).

Furthermore we have included the reasoning outputs for each of the open weight reasoning models. These are provided for transparency, despite no analyses being performed upon them (due to the poor quality of responses from the open models).

## C EXTENDED RELATED WORK

Since the advent of LLMs, many groups have explored their compositional components. Notably, this has included investigating the ability to answer compositional subproblems without successfully answering the overall problem (Press et al., 2023), evaluating linguistic compositional generation (Kim & Linzen, 2020), and evaluating compositional generation in images (Liu et al., 2022). No existing work has looked at the composition of image-like propositions in LLMs. Furthermore, research on how LLMs think in general (Shiffrin & Mitchell, 2023; Liu et al., 2025; Lombrozo, 2024; Pavlick, 2023) and how they may access their own processes Plunkett et al. (2025); Betley et al. (2025) is a crucial stepping stone for further understanding how LLMs may perform imagery tasks via propositional reasoning.

## D EXTENDED PERFORMANCE EVALUATION - HUMANS

### D.1 GRADE WEIGHTING

In our initial work on grading the task we ran into two key issues: first, the issue of subjectivity as described previously; second, some answers were extremely literal and, as such, did not represent a new construction. Our initial plan was to grade similarly to Finke et al. (1989), but the subjectivity issue necessitated us exploring different options.

After recruiting our first set of subjects, we discovered a key issue with the responses. Namely, hyper-literal responses (e.g., ‘bd’ after asking subjects to imagine a ‘b’ next to a ‘d’ and pressing them together) were graded very highly. We attempted to control for this by instructing subjects to rate such examples poorly, but, unfortunately, these were routinely graded highly. Our solution to this issue was to have the authors grade all 1911 responses in addition to the 376 naïve subjects.

Almost all responses had 5 subject ratings, a few responses had 6, a very small number 7, and a single response 4 due to the random distribution methods of Qualtrics XM. In all cases we generated a ‘normal\_score’ from the mean of all of the responses. In addition, we generated an ‘expert\_score’ from the mean of the authors’ ratings. Our final ‘overall\_score’ was the average of the ‘normal\_score’

and the ‘expert\_score’. All scores for all responses used in grading are available in our dataset (see Appendix B).

The subject ratings were distributed (Supplemental Figure S8) very heavily towards “Not at all” (or a grade of 1) due to most examples being difficult to justify (due to misconstructions, possible confusion in the case of humans, or possible hallucinations in the case of LLMs). The expert scores (Supplemental Figure S9) were distributed similarly, but with a noticeably higher occurrence of “Completely” (or a grade of 5). Knowledge of the creation of the items and their intended canonical result, along with a reduced bias towards the drawn representations of the intended mental image likely account for this.

## D.2 DIFFICULTY ANALYSIS

Concurrently with the experimental task, we asked all participants to report how clear they found the instructions, as well as how identifiable they found the final mental image (both on a 5 point scale). These ratings as well as their standard deviations as a measure of consistency, along with the ratio of unique responses given to each answer, the number of instruction steps, and the number of imagined objects, were used to rank each of the instruction sets on the following weighted difficulty scale:

$$\begin{aligned} \text{Item Difficulty} = & (0.20 \times \text{Total Instruction Steps}) \\ & + (0.20 \times \text{Total Objects}) \\ & + [0.15 \times (6 - \text{Mean Clarity Ratings})] \\ & + [0.15 \times (6 - \text{Mean Identifiability Ratings})] \\ & + (0.10 \times \text{Clarity Ratings Standard Deviation}) \\ & + (0.10 \times \text{Identifiability Ratings Standard Deviation}) \\ & + (0.10 \times \text{Unique Response Ratio}) \end{aligned}$$

$$\text{Unique Response Ratio} = \frac{\text{Unique Responses Per Label}}{\text{Total Responses Per Label}}$$

Overall, we found that our set of instructions had a wide range of difficulty levels (see Supplemental Figure S11 for the distribution). We confirmed that the items that we designed to be harder (e.g., constructing a “computer mouse”) indeed came out ranked as the most difficult, whereas the easiest ones (e.g., constructing a “ladder”) were ranked as the easiest.

We can validate this by viewing the mean score given to each instruction set by the graders, and seeing a broad distribution (Supplemental Figure S10).

## D.3 VVIQ ANALYSIS

The VVIQ scale range is 16 (minimum) to 80 (maximum). Subjects had a mean VVIQ score of 55.8, confirming that our sample was normal given recent large sampling efforts (Wright et al., 2024). We did not find any correlation between VVIQ scores and subjects’ performance (Pearson’s  $r = -0.17$ ,  $p = .0942$ ). If anything, there was a negative trend, suggesting that imagery capacity as measured by the VVIQ could not predict performance in a task designed to measure mental imagery. See Supplemental Figure S12.

Of the 100 subjects we tested, one subject qualified as a true aphantasic (VVIQ score of 16, the minimum). This subject, however, had the 5th highest score of all human subjects. While this constitutes a single data point (all other subjects had higher VVIQ scores), it raises the question of how this subject was able to complete the task. Recent data has shown that aphantasics can complete imagery tasks surprisingly well (Blomkvist, 2023; Kay et al., 2024; Pounder et al., 2022), even if the exact way in which they accomplish this or whether they use a single strategy across tasks is still unclear.

There were three subjects who qualified as low-imagers (or weak aphantasics) scoring between 17 and 32 on the VVIQ (23, 29, 29). Two of the subjects performed around the median score for humans (53rd and 56th), while the third was the 15th highest scoring individual in our dataset.

Lastly, we had seven subjects who had very high imagery (or hyperphantasics) scoring between 75 and 80 (the highest) on the VVIQ (one scored 77 the rest 80). These subjects had very mixed performance with three subjects performing above the median (18th, 20th, and 24th), and four subjects performing well below the median, and in a couple cases getting close to the bottom performance (77th, 81st, 91st, and 94th).

The high performance exhibited by the aphantasic subjects and the most advanced LLMs, in addition to the lack of correlation between imagery capacity (measured via VVIQ) and performance in the task, offers further evidence that mental imagery may operate in a propositional format. At the very least, this supposedly gold standard for probing pictorial imagining may not be as well suited for the task as generations of cognitive psychologists have thought. Naturally, much more data and analysis is needed to cement this conclusion. The current experiments with LLMs, and future ones as well, may help further our understanding of how aphantasics are able to accomplish these and other tasks. (For one possible explanation appealing to spatial imagery, see section 4 in the main text).

## E EXTENDED PERFORMANCE EVALUATION - LLMs

### E.1 REASONING VARIATION

In addition to the selection of models we tested with ‘reasoning\_effort’ set to ‘high’, we tested the best performing reasoning models on ‘low’ and ‘medium’ (and GPT-5 on ‘minimal’), as well as two other models on ‘medium’ (see Supplemental Table S3).

Overall we saw that as reasoning token and time allocations decreased, so did the performance (o3 ‘high’ vs. ‘medium’: 7.7% difference [ $\chi^2 = 5.401$ ,  $p = .0201$ ,  $CI = [0.011, 0.144]$ ]; vs. ‘low’ 10.2% difference [ $\chi^2 = 9.513$ ,  $p = .0020$ ,  $CI = [0.035, 0.169]$ ]; GPT-5 ‘high’ vs. ‘medium’: 7.5% difference [ $\chi^2 = 4.594$ ,  $p = 0.0320$ ,  $CI = [0.005, 0.145]$ ]; vs. ‘low’: 16.4% difference [ $\chi^2 = 22.084$ ,  $p < .00001$ ,  $CI = [0.094, 0.235]$ ]; vs. ‘minimal’: 26.2% difference [ $\chi^2 = 55.522$ ,  $p < .00001$ ,  $CI = [0.193, 0.332]$ ]; additionally see Supplemental Figure S4 and S5). One interesting data point, however, was the lack of any significant difference between ‘high’ and ‘medium’ in o3 with GPT-image-1 (‘high’ vs. ‘medium’: 0.5% difference [ $\chi^2 = 0.008$ ,  $p = .9281$ ,  $CI = [-0.06, 0.07]$ ). This may hint at the possibility that the image paradigm has, despite models overall lower performance, the potential to provide some support solving this task. The issues with compositional generation inherent to image generation models, however, may hinder it overall (Huang et al., 2023). We provide statistics between humans and our reasoning model variations in Appendix E.4.2.

### E.2 REASONING UNDER UNCERTAINTY

One remarkable result we found was the lack of capability for LLMs to answer with uncertainty (and yet, it was unsurprising given well-known limitations of LLMs). We noted 54 occurrences of humans responding some form of “I don’t know” to an instruction set, and 0 occurrences in the LLM responses. It is highly possible that LLMs provide responses even when great uncertainty exists (especially in our hardest instruction sets). This is an area worth exploring in further analyses on how LLMs succeed or fail at the task (Brahman et al., 2024; Kadavath et al., 2022; Malinin & Gales, 2021).

Interestingly, when asked to report the imagined object when given no instructions, open models reported answers like “blank slate” or “artificial neuron” implying some ability to give ambiguous responses in cases of uncertainty. The impact of this on our task needs to be explored further by future researchers.

### E.3 MODEL TEMPERATURE

In our initial testing, with the exception of Gemini 2.5 Pro (where we set the temperature to 0.1), all reasoning models were restricted to high temperatures by their respective APIs (1.0 for Claude

and OpenAI models). After considering that the performance of Gemini 2.5 Pro (well below the other frontier reasoning models) may be due to the low temperature, we performed a new test using Gemini 3 Pro.

Temperature has been shown to meaningfully affect reasoning outputs (Wang et al., 2024a), though on many tasks it does not necessarily improve the results (Renze & Guven, 2024). We performed a hyperparameter search of the ‘temperature’ parameter using values 0.1, 0.55, and 1.0 upon the release of Gemini 3 Pro. We were curious if modification in temperature would allow the model to explore more creative paths to the correct answer and succeed more often (Turing, 1950). We found no significant difference between any of the temperature values tested. See Appendix E.5.

## E.4 EXTENDED STATISTICAL ANALYSIS

### E.4.1 STANDARD PARADIGM

Humans vs. . . . :

- o3: -9.4% difference,  $\chi^2 = 28.631$ ,  $p < .00001$ ,  $CI = [-0.128, -0.06]$
- o3 with GPT-image-1: -0.6% difference,  $\chi^2 = 0.143$ ,  $p = .7057$ ,  $CI = [-0.037, 0.024]$
- o3-Pro: -11.9% difference,  $\chi^2 = 45.76$ ,  $p < .00001$ ,  $CI = [-0.153, -0.086]$
- GPT-4.1: 12.2% difference,  $\chi^2 = 32.987$ ,  $p < .00001$ ,  $CI = [0.08, 0.164]$
- GPT-4.1 with GPT-image-1: 16.4% difference,  $\chi^2 = 59.482$ ,  $p < .00001$ ,  $CI = [0.123, 0.206]$
- ChatGPT-4o: 12.8% difference,  $\chi^2 = 35.86$ ,  $p < .00001$ ,  $CI = [0.086, 0.17]$
- o4-mini: 1.7% difference,  $\chi^2 = 0.577$ ,  $p = .4477$ ,  $CI = [-0.025, 0.059]$
- Gemini 2.5 Pro: 12.2% difference,  $\chi^2 = 32.987$ ,  $p < .00001$ ,  $CI = [0.08, 0.164]$
- Gemini 2.0 Flash: 16.7% difference,  $\chi^2 = 61.741$ ,  $p < .00001$ ,  $CI = [0.126, 0.209]$
- Gemini 2.0 Flash with Images: 21.6% difference,  $\chi^2 = 53.296$ ,  $p < .00001$ ,  $CI = [0.16, 0.272]$
- Claude Sonnet 4: 13% difference,  $\chi^2 = 37.392$ ,  $p < .00001$ ,  $CI = [0.088, 0.172]$
- Claude Opus 4.1: 1.8% difference,  $\chi^2 = 0.299$ ,  $p = .5845$ ,  $CI = [-0.042, 0.077]$
- GPT-5: -12.3% difference,  $\chi^2 = 33.302$ ,  $p < .00001$ ,  $CI = [-0.163, -0.082]$
- Gemini 3 Pro: -18.24% difference,  $\chi^2 = 108.103$ ,  $p < .00001$ ,  $CI = [-0.214, -0.151]$
- DeepSeek R1: 15.7% difference,  $\chi^2 = 28.182$ ,  $p < .00001$ ,  $CI = [0.099, 0.216]$
- gpt-oss-120b: 17.9% difference,  $\chi^2 = 36.444$ ,  $p < 0.00001$ ,  $CI = [0.121, 0.236]$
- Qwen 3: 23.3% difference,  $\chi^2 = 61.874$ ,  $p < .00001$ ,  $CI = [0.177, 0.288]$
- Qwen 3 VL: 15.2% difference,  $\chi^2 = 26.355$ ,  $p < .00001$ ,  $CI = [0.094, 0.211]$

### E.4.2 REASONING VARIATIONS

Humans vs. . . . :

- o3 ‘high’: -9.4% difference,  $\chi^2 = 28.631$ ,  $p < .00001$ ,  $CI = [-0.128, -0.06]$
- o3 ‘medium’: -1.7% difference,  $\chi^2 = 0.273$ ,  $p = .6014$ ,  $CI = [-0.076, 0.042]$
- o3 ‘low’: 0.8% difference,  $\chi^2 = 0.273$ ,  $p = .8349$ ,  $CI = [-0.051, 0.067]$
- o3 with GPT-image-1 ‘high’: -0.6% difference,  $\chi^2 = 0.143$ ,  $p = .7057$ ,  $CI = [-0.037, 0.024]$
- o3 with GPT-image-1 ‘medium’: -0.1% difference,  $\chi^2 = 0$ ,  $p = 1$ ,  $CI = [-0.06, 0.057]$
- o3-Pro ‘high’: -11.9% difference,  $\chi^2 = 45.76$ ,  $p < .00001$ ,  $CI = [-0.153, -0.086]$
- o4-mini ‘high’: 1.7% difference,  $\chi^2 = 0.577$ ,  $p = .4477$ ,  $CI = [-0.025, 0.059]$
- o4-mini ‘medium’: 5.8% difference,  $\chi^2 = 7.209$ ,  $p = .0073$ ,  $CI = [0.015, 0.1]$

- GPT-5 ‘high’: -12.3% difference,  $\chi^2 = 33.302$ ,  $p < .00001$ ,  $CI = [-0.163, -0.082]$
- GPT-5 ‘medium’: -4.8% difference,  $\chi^2 = 2.441$ ,  $p = .1182$ ,  $CI = [-0.106, 0.011]$
- GPT-5 ‘low’: 4.2% difference,  $\chi^2 = 1.854$ ,  $p = .1733$ ,  $CI = [-0.018, 0.101]$
- GPT-5 ‘minimal’: 14% difference,  $\chi^2 = 22.151$ ,  $p < .00001$ ,  $CI = [0.081, 0.198]$

## E.5 TEMPERATURE VARIATIONS

### Gemini 3 Pro:

- Temperature of 0.1 vs. Temperature of 0.55: 2.6% difference,  $\chi^2 = 0.379$ ,  $p = .538$ ,  $CI = [-0.049, 0.101]$
- Temperature of 0.1 vs. Temperature of 1.0: -0.14% difference,  $\chi^2 = 0.097$ ,  $p = .7556$ ,  $CI = [-0.088, 0.059]$
- Temperature of 0.55 vs. Temperature of 1.0: -4% difference,  $\chi^2 = 1.038$ ,  $p = .3082$ ,  $CI = [-0.115, 0.034]$

## F FUTURE WORK

This work has several future steps given its impact both within cognitive science as well as artificial intelligence.

First, in humans, aphantasics lack voluntary visual mental imagery, but report little-to-no issues in other areas of everyday life; often times living without knowing of the condition at all (Larner et al., 2024). We suggest a follow-up study on the strategies and techniques used by aphantasics in comparison to those used by LLMs. The lack of visual imagery parallels the inability for visual imagery inherent to LLMs, and by studying both groups, it may be possible to learn more about the need for pictorial imagery or the lack there-of to perform compositional tasks like the one we tested.

Second, as multimodal auditory, vision, and language models continue to advance, the capabilities of these models surely will as well. We propose continuing to evaluate the performance of the leading frontier models on our paradigm. Currently, given the bespoke nature of our stimuli, our task is not contained within the training data of any model as of now and, as such, is not subject to data contamination issues. However, as time passes this risk continues to increase. Creating more items in this kind of task requires certain ingenuity but they are sufficiently straightforward that new ones can be devised *ad hoc*. Further model evaluation should include tasks hidden from public datasets to truly measure advancement in propositional reasoning.

Third, humans provided a great limitation to the creation of trials that would serve for further exploring LLMs capacities. The general rule is 7 plus or minus 2 (or even less) objects can be worked with at once in human working memory (Miller, 1956; Farrington, 2011). LLMs are only limited by their contexts, which can hold vastly more information than any human. Without this limitation, it is unknown the extent of LLMs propositional reasoning capacity. As such, trials with many more than 3-5 steps and many more than 4 objects may be created, and, furthermore, may be necessary for future evaluation given GPT-5 and the o3 family’s performance on the existing items. Conversely, we do not know to what extent our task necessitates working memory. It may be entirely possible for humans to work through an arbitrary number of iterative instructions, with an arbitrary number of components (overall, not per-step), given that each step creates a new imaginary scene (and therefore humans may only have to keep the previously imagined scene, and any new information, in mind).

Finally, in the future, as models progressively get stronger, open weight models that perform well enough on this task to compete with the GPT-5 and o3 family may exist. If this happens, we propose mechanistic approaches that look inside the models and directly examine the formats of representation. Can we find direct evidence of propositional reasoning (or learned iconic representations or a distinct spatial imagery capacity) by examining the weights of the models McCoy et al. (2019); Piantadosi et al. (2024)? Unfortunately, our results with some of the largest current open models, this possibility is not available since open models significantly underperform.

## G TECHNICAL SETUP

All model prompting was done through the respective APIs of the models' parent company in Python. Models were run at least once in multiple-context with most models being run at least once in both single-context and multiple-context. After determining that there was no statistical difference between the two paradigms, any subsequent runs of models were run in multiple-context (due to the decreased cost of inference because of less input token usage).

Our exact runs of model paradigms are as follows:

- Claude Opus 4.1, multiple-context: 1
- Claude Sonnet 4, multiple-context: 1
- Claude Sonnet 4, single-context: 1
- Gemini 2.0 Flash, multiple-context: 1
- Gemini 2.0 Flash, single-context: 1
- Gemini 2.0 Flash images, multiple-context: 1
- Gemini 2.5 Pro, multiple-context: 1
- Gemini 2.5 Pro, single-context: 1
- ChatGPT-4o, multiple-context: 1
- ChatGPT-4o, single-context: 1
- GPT-4.1, multiple-context: 1
- GPT-4.1, single-context: 1
- GPT-4.1 with GPT-image-1, multiple-context: 1
- GPT-4.1 with GPT-image-1, single-context: 1
- GPT-5, high reasoning, multiple-context: 2
- GPT-5, medium reasoning, multiple-context: 1
- GPT-5, low reasoning, multiple-context: 1
- GPT-5, minimal reasoning, multiple-context: 1
- o3, high reasoning, multiple-context: 2
- o3, high reasoning, single-context: 1
- o3, medium reasoning, multiple-context: 1
- o3, low reasoning, multiple-context: 1
- o3-Pro, high reasoning, multiple-context: 2
- o3-Pro, high reasoning, single-context: 1
- o3 with GPT-image-1, high reasoning, multiple-context: 4
- o3 with GPT-image-1, medium reasoning, multiple-context: 1
- o4-mini, high reasoning, multiple-context: 1
- o4-mini, high reasoning, single-context: 1
- o4-mini, medium reasoning, multiple-context: 1
- o4-mini, medium reasoning, single-context: 1
- Gemini 3 Pro, high thinking, temperature 1.0, multiple-context: 1
- Gemini 3 Pro, high thinking, temperature 0.55, multiple-context: 1
- Gemini 3 Pro, high thinking, temperature 0.1, multiple-context: 1
- DeepSeek R1, default reasoning, multiple-context: 1
- Qwen 3, default reasoning, multiple-context: 1
- Qwen 3 VL, default reasoning, multiple-context: 1
- gpt-oss-120b, high reasoning, multiple-context: 1

1242 The strongest OpenAI reasoning models were run a single additional time with variations on the  
1243 'reasoning\_effort' parameter as described in Appendix E.1. Our reported data in all other sections is  
1244 based on the 'reasoning\_effort' parameter being set to 'high'.

1245 For all models which allowed modification in their 'temperature' parameter, we set it to 0.1 (rea-  
1246 soning models from OpenAI and Anthropic do not allow modification to temperature). All other  
1247 hyperparameters were left at their default value.

1249 For OpenAI, we used the openai package, version 1.76.2; for Gemini, the google-genai package  
1250 version 1.14.0 (for Gemini 3 Pro this was updated to 1.51.0); for Claude, the anthropic package  
1251 version 0.52.2. We used the Miniconda environment manager to create a Python 3.12.9 environment,  
1252 and the complete frozen package list ('python\_env.yml') is available in our repository (see Appendix  
1253 B).

1254 For open models (including gpt-oss-120b) we used the openai package (same version as before) and  
1255 the API platform OpenRouter.

1256 Our prompt processing pipeline was run on a 2019 Razer Blade Stealth running Arch Linux with 16  
1257 GB of RAM, an 8 core Intel CPU (i7-8565U), and no dedicated GPU.

1258 All data collected from models totaled around \$1000 US in cost. The exact versions of models is  
1259 listed in Table S2.

1261 Data pre-processing was performed in a Jupyter Notebook file. We provide .md and .html versions  
1262 of the output in addition to the raw file for convenience.

1263 Statistical analyses were performed using R 4.3.3 in PyCharm with the R plugin installed. Mini-  
1264 conda was also used to create a replicable environment and the frozen package list ('r\_env.yml') is  
1265 available in our repository. Our analyses were performed within an R Markdown script. We provide  
1266 .html and .pdf exports for simplified viewing.

1267  
1268  
1269  
1270  
1271  
1272  
1273  
1274  
1275  
1276  
1277  
1278  
1279  
1280  
1281  
1282  
1283  
1284  
1285  
1286  
1287  
1288  
1289  
1290  
1291  
1292  
1293  
1294  
1295

H SUPPLEMENTAL FIGURES

1296  
1297  
1298  
1299  
1300  
1301  
1302  
1303  
1304  
1305  
1306  
1307  
1308  
1309  
1310  
1311  
1312  
1313  
1314  
1315  
1316  
1317  
1318  
1319  
1320  
1321  
1322  
1323  
1324  
1325  
1326  
1327  
1328  
1329  
1330  
1331  
1332  
1333  
1334  
1335  
1336  
1337  
1338  
1339  
1340  
1341  
1342  
1343  
1344  
1345  
1346  
1347  
1348  
1349

	Step 1	Step 2	Step 3	Step 4	Result
Instructions	Generate an image with two capital letter "B" next to each other.	From there, modify the image with the left figure mirrored so that it points left.	From there, modify the image with the two figures aligned such that the two vertical lines are overlaid.	From there, modify the image with a lowercase letter "v" affixed to the middle of the top of the figure.	Canonical form: Butterfly
Mental Image					"Butterfly"

Figure S1: An example image generation output from GPT-image-1 in combination with o3. No seed image was given to the model, but subsequent steps retained the previous image and asked for its modification.

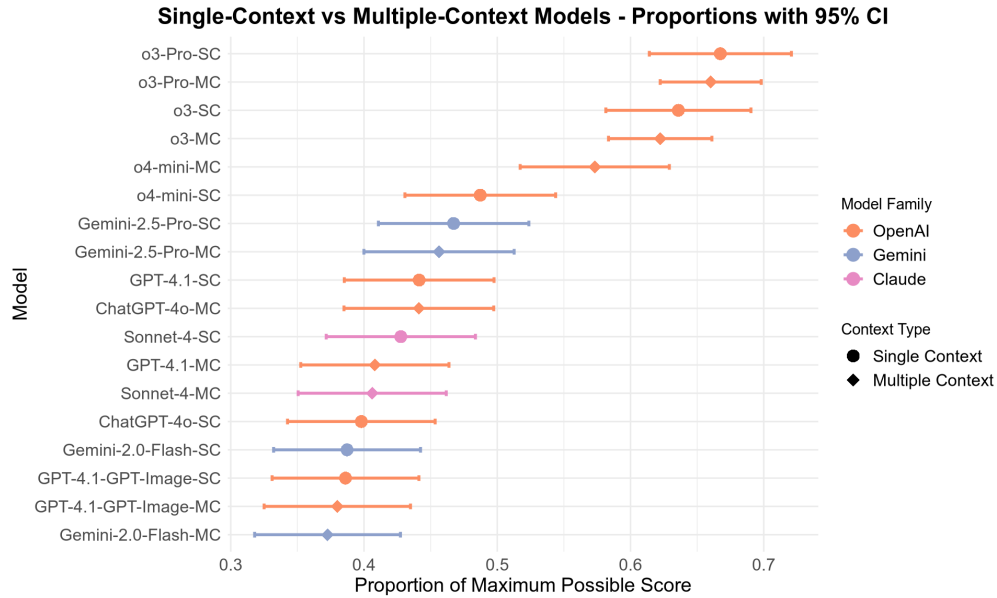


Figure S2: 95% confidence intervals showing the differences between Single-Context and Multiple-Context. Single-Context has a slight, non-significant edge in most cases. All context variant comparisons were non-significant after correcting for multiple-comparisons.

1350  
1351  
1352  
1353  
1354  
1355  
1356  
1357  
1358  
1359  
1360  
1361  
1362  
1363  
1364  
1365  
1366  
1367  
1368  
1369  
1370  
1371  
1372  
1373  
1374  
1375  
1376  
1377  
1378  
1379  
1380  
1381  
1382  
1383  
1384  
1385  
1386  
1387  
1388  
1389  
1390  
1391  
1392  
1393  
1394  
1395  
1396  
1397  
1398  
1399  
1400  
1401  
1402  
1403

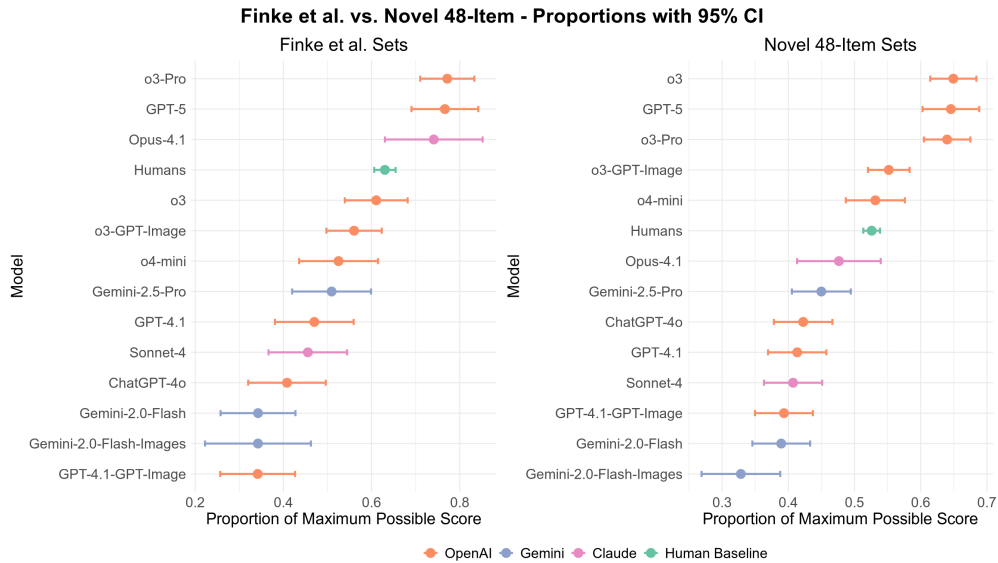


Figure S3: Separated 95% proportions of maximum possible score between Finke et al. Items (left) and 48 Novel Items (right).

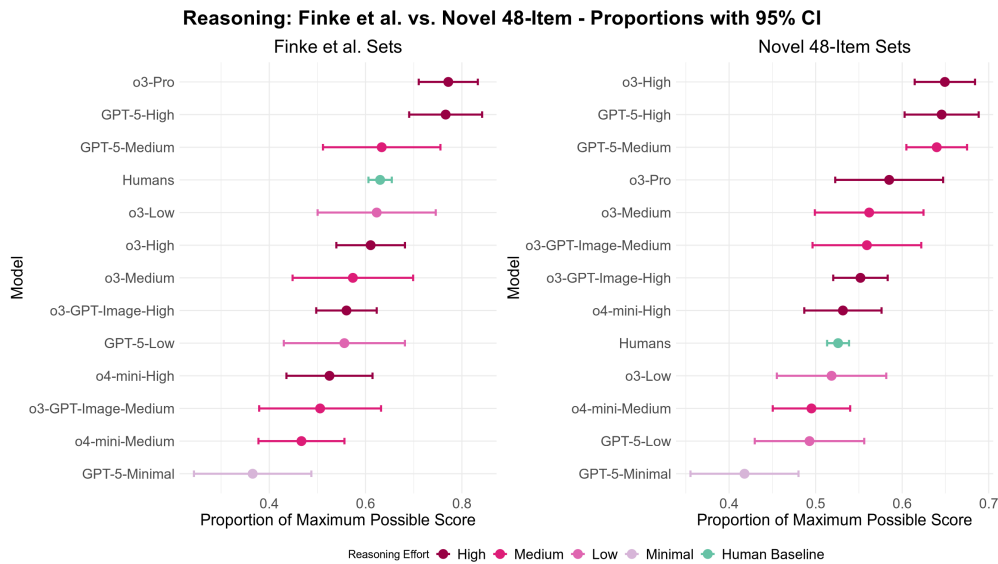


Figure S4: Hyperparameter comparison of results (95% confidence intervals of proportions of maximum possible score) after modifying 'reasoning\_effort' parameter in OpenAI Large Language Reasoning Models. Human baseline is included. Generally, as reasoning effort (token generation amount) increases, so does performance. Results are separated by Finke et al. Items (left) and 48 Novel Items (right).

1404  
1405  
1406  
1407  
1408  
1409  
1410  
1411  
1412  
1413  
1414  
1415  
1416  
1417  
1418  
1419  
1420  
1421  
1422  
1423  
1424  
1425  
1426  
1427  
1428  
1429  
1430  
1431  
1432  
1433  
1434  
1435  
1436  
1437  
1438  
1439  
1440  
1441  
1442  
1443  
1444  
1445  
1446  
1447  
1448  
1449  
1450  
1451  
1452  
1453  
1454  
1455  
1456  
1457

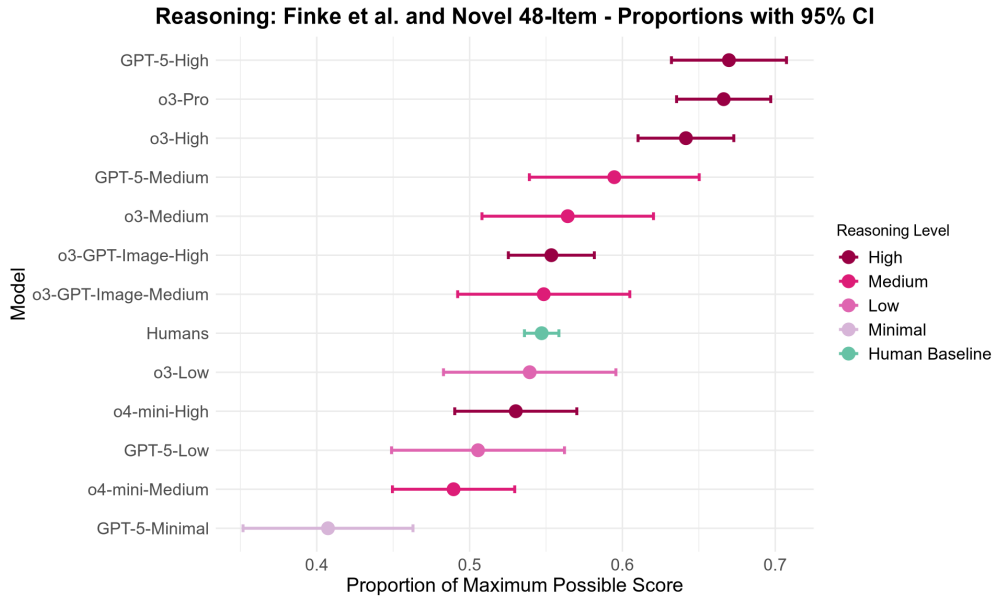


Figure S5: Hyperparameter comparison of collapsed results (95% confidence intervals of proportions of maximum possible score) after modifying 'reasoning\_effort'.

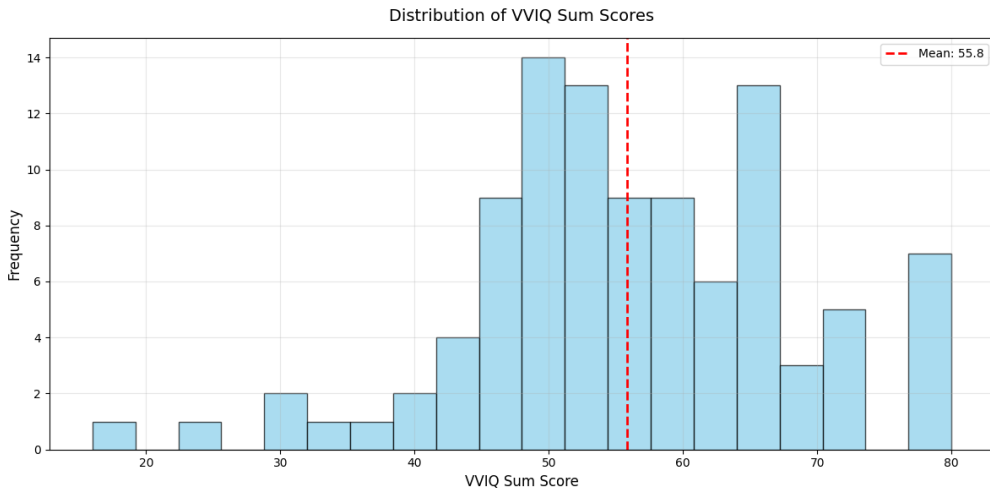


Figure S6: The distribution of VVIQ scores for our 100 human subjects. 1 subject qualified as an aphantasic under the strictest condition (VVIQ = 16). The characteristic left skew of the distribution is clear.

1458  
 1459  
 1460  
 1461  
 1462  
 1463  
 1464  
 1465  
 1466  
 1467  
 1468  
 1469  
 1470  
 1471  
 1472  
 1473  
 1474  
 1475  
 1476  
 1477  
 1478  
 1479  
 1480  
 1481  
 1482  
 1483  
 1484  
 1485  
 1486  
 1487  
 1488  
 1489  
 1490  
 1491  
 1492  
 1493  
 1494  
 1495  
 1496  
 1497  
 1498  
 1499  
 1500  
 1501  
 1502  
 1503  
 1504  
 1505  
 1506  
 1507  
 1508  
 1509  
 1510  
 1511

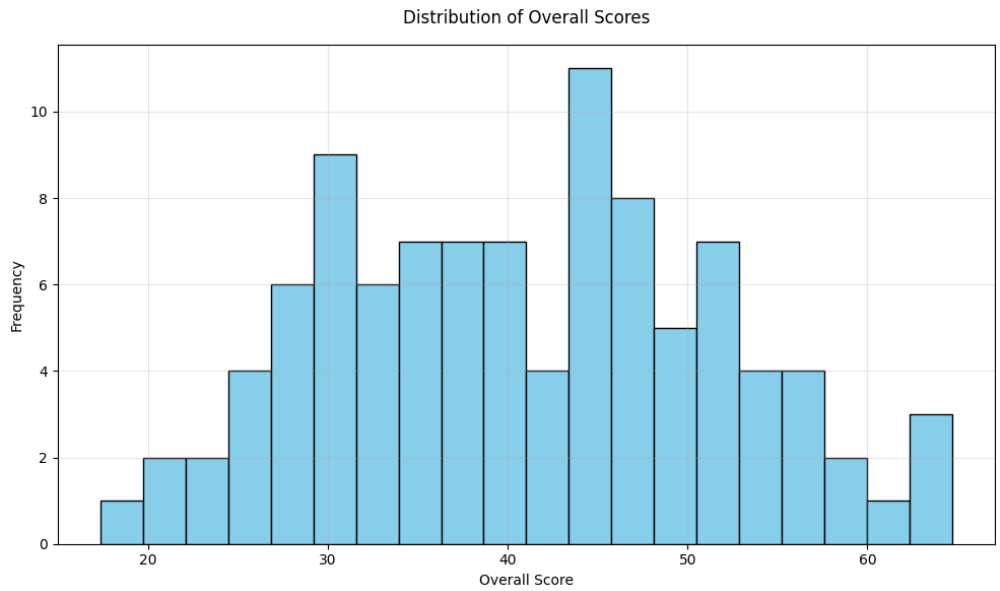


Figure S7: The distribution of overall graded scores for the 100 human subjects. As the subset of questions given to each subject was random, the overall difficulty of each set was not guaranteed and therefore some noise in the score distribution is expected.

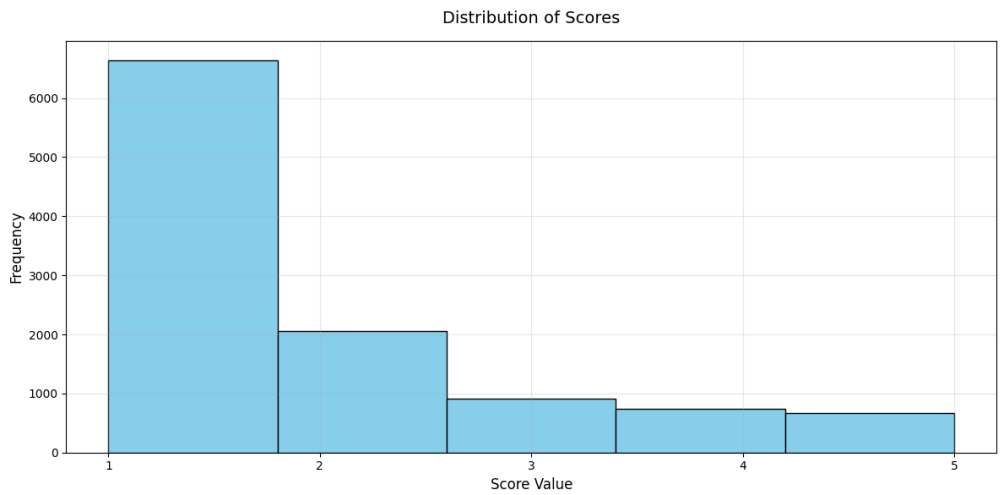


Figure S8: The distribution of scores given to unique answers by the 376 crowd-sourced subjects.  $\approx 5$  per each of the 1911 unique responses. Experts gave more high ratings than the random subjects.

1512  
 1513  
 1514  
 1515  
 1516  
 1517  
 1518  
 1519  
 1520  
 1521  
 1522  
 1523  
 1524  
 1525  
 1526  
 1527  
 1528  
 1529  
 1530  
 1531  
 1532  
 1533  
 1534  
 1535  
 1536  
 1537  
 1538  
 1539  
 1540  
 1541  
 1542  
 1543  
 1544  
 1545  
 1546  
 1547  
 1548  
 1549  
 1550  
 1551  
 1552  
 1553  
 1554  
 1555  
 1556  
 1557  
 1558  
 1559  
 1560  
 1561  
 1562  
 1563  
 1564  
 1565

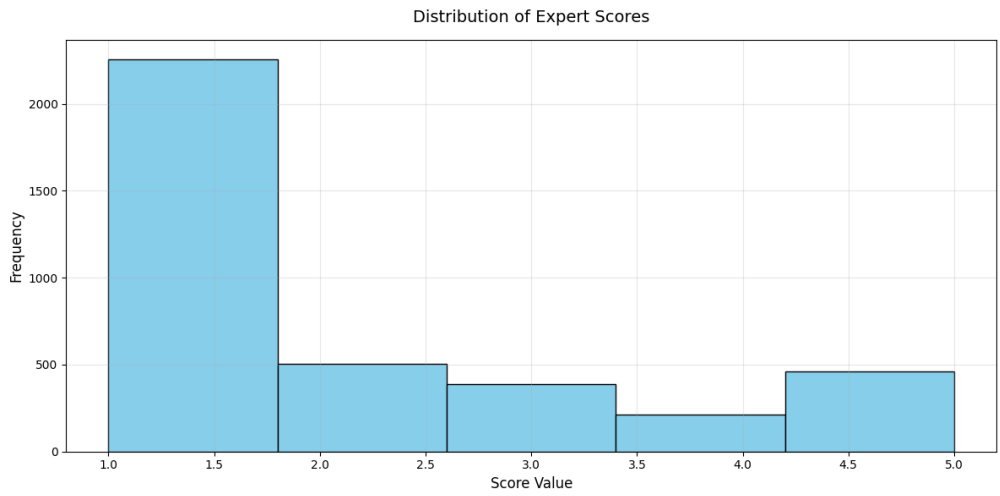
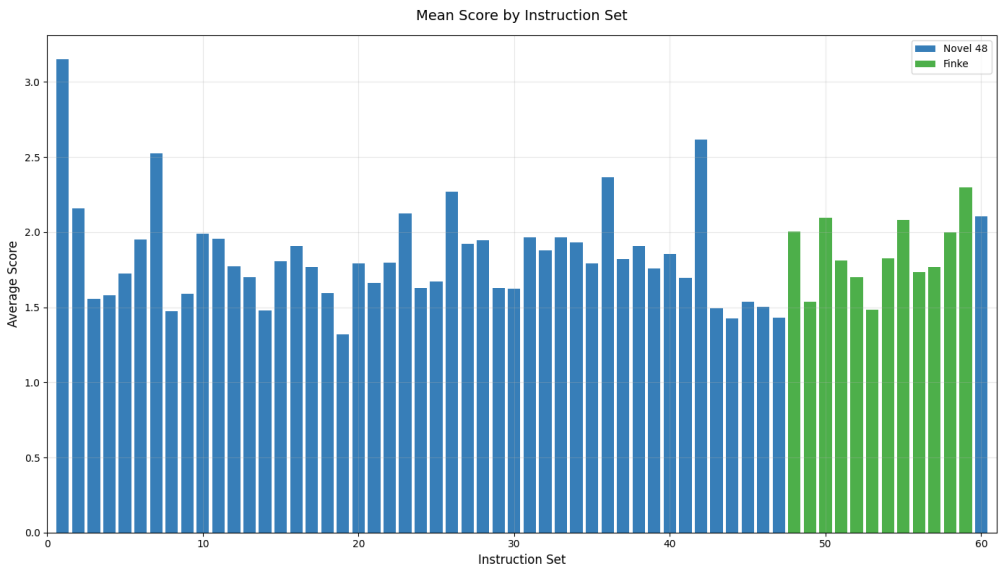


Figure S9: The distribution of scores given to unique answers by the 2 expert subjects. 2 to each of the 1911 unique responses.



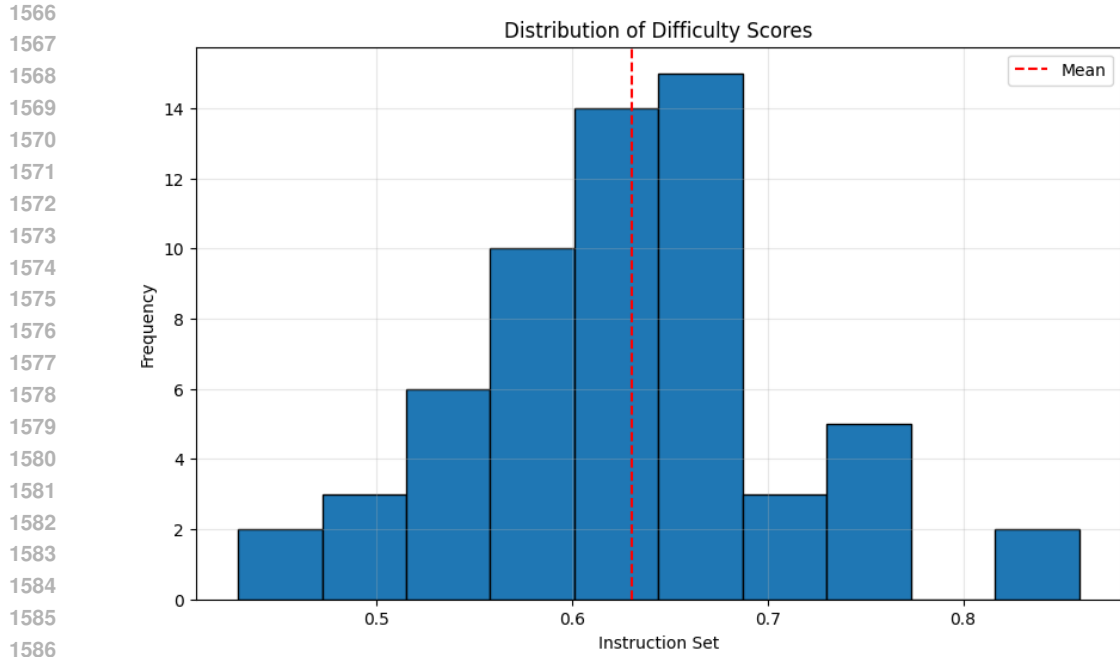


Figure S11: Distribution of calculated difficulty scores per instruction set. Our instruction sets showed strong variance of difficulty.

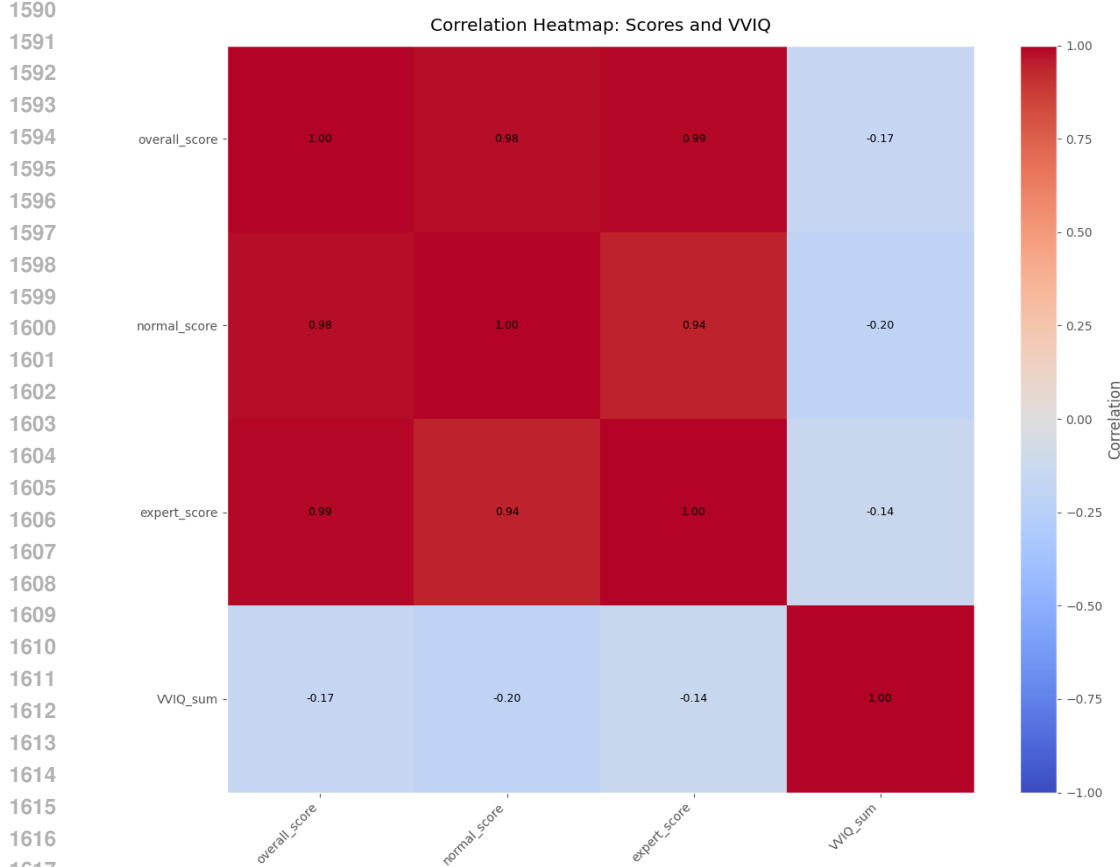


Figure S12: Correlation between VVIQ score sum, 'overall\_score', 'normal\_score', and 'expert\_score' (see Appendix D.1 for terminology explanation).

## I SUPPLEMENTAL TABLES

Table S1: Model selection and features. For OpenAI reasoning models, ‘reasoning\_effort’ was set to ‘high’ (as shown) and, for the models indicated, GPT-image-1 was integrated. For Gemini models, default parameters regarding reasoning were retained and native image generation tools were used. For Claude models a reasoning token budget was manually given (well above what was ever allocated). This table only shows the primarily graded models, not the reasoning variations in our reasoning model effort analysis.

Model	Reasoning	Image Generation
GPT-5	High	No
o3-Pro	High	No
o3	High	Yes
o4-mini	High	No
ChatGPT-4o	No	No
GPT-4.1	No	Yes
Gemini 2.5 Pro	Dynamic	No
Gemini 2.0 Flash	No	Yes
Claude Sonnet 4	4000t	No
Claude Opus 4.1	9000t	No

Table S2: Model Versions. Model versions used in our analysis. When possible exact dated versions are given, if no such version is available the date of usage was also provided.

Model	Version
GPT-5	gpt-5-2025-08-07
o3	o3-2025-04-16
o3-Pro	o3-pro-2025-06-10
o4-mini	o4-mini-2025-04-16
ChatGPT-4o	chatgpt-4o-latest (July 2025)
GPT-4.1	gpt-4.1-2025-04-14
GPT-image-1	gpt-image-1-2025-04-23
Gemini 2.0 Flash	gemini-2.0-flash (February 2025)
2.0 Flash Image Preview	gemini-2.0-flash-preview-image-generation (May 2025)
Gemini 2.5 Pro	gemini-2.5-pro-preview-05-06
Claude Sonnet 4	claude-sonnet-4-20250514
Claude Opus 4.1	claude-opus-4-1-20250805
Gemini 3 Pro	gemini-3-pro-preview (November 2025)
DeepSeek R1	deepseek-r1-0528
Qwen 3	qwen3-235b-a22b-thinking-2507
Qwen 3 VL	qwen3-vl-235b-a22b-thinking
gpt-oss-120b	gpt-oss-120b

Table S3: Reasoning Variations. Reasoning level variations used for reasoning analysis.

Model	Reasoning Levels Used
GPT-5	Minimal, Low, Medium, High
o3-Pro	High
o3	Low, Medium, High
o3 with GPT-image-1	Medium, High
o4-mini	Medium, High

Table S4: Results Breakdown. Models in bold indicate highest performer in the group. The human baseline is in green. Models in purple surpass the human baseline significantly [ $** p < .01$ ,  $*** p < .001$ ]. Models in blue are not significantly [ $^{ns}$ ] different from the human baseline (i.e., at human level).

Agent	Score	Max Possible Score	Proportion
<i>Finke et al. Items</i>			
Humans	961.096	1525	0.6302
o3 <sup>ns</sup>	109.900	180	0.6106
o3 + GPT-image-1	134.483	240	0.5603
<b>o3-Pro<sup>***</sup></b>	<b>138.908</b>	<b>180</b>	<b>0.7717</b>
GPT-4.1	56.407	120	0.4701
GPT-4.1 + GPT-image-1	41.000	120	0.3417
o4-mini	63.008	120	0.5251
Gemini 2.5 Pro	61.125	120	0.5094
Gemini 2.0 Flash	41.100	120	0.3425
Gemini 2.0 Flash + Images	20.538	60	0.3423
Claude Sonnet 4	54.652	120	0.4554
Claude Opus 4.1 <sup>ns</sup>	44.467	60	0.7411
GPT-5 <sup>**</sup>	91.950	120	0.7663

Table S5: Novel 48-Item Expansion Results Breakdown. Models in bold indicate highest performer in the group. The human baseline is in green. Models in purple surpass the human baseline significantly [ $** p < .01$ ,  $*** p < .001$ ]. Models in blue are not significantly [ $^{ns}$ ] different from the human baseline (i.e., at human level).

Agent	Score	Max Possible Score	Proportion
<i>48 Novel Items</i>			
Humans	3137.120	5965	0.5259
<b>o3<sup>***</sup></b>	<b>467.490</b>	<b>720</b>	<b>0.6493</b>
o3 + GPT-image-1 <sup>ns</sup>	529.699	960	0.5518
o3-Pro <sup>***</sup>	460.713	720	0.6399
GPT-4.1	198.455	480	0.4134
GPT-4.1 + GPT-image-1	188.827	480	0.3934
o4-mini <sup>ns</sup>	255.123	480	0.5315
Gemini 2.5 Pro	215.949	480	0.4499
Gemini 2.0 Flash	186.882	480	0.3893
Gemini 2.0 Flash + Images	78.807	240	0.3284
Claude Sonnet 4	195.488	480	0.4073
Claude Opus 4.1 <sup>ns</sup>	114.352	240	0.4765
GPT-5 <sup>***</sup>	309.873	480	0.6456